HHS Public Access

Author manuscript

Neuron. Author manuscript; available in PMC 2019 December 19.

Published in final edited form as:

Neuron. 2018 December 19; 100(6): 1401–1413.e6. doi:10.1016/j.neuron.2018.10.034.

MERKEL CELLS ACTIVATE SENSORY NEURAL PATHWAYS THROUGH ADRENERGIC SYNAPSES

Benjamin U. Hoffman[1,2], **Yoshichika Baba**[1], **Theanne N. Griffith**[1], **Eugene V. Mosharov**[3], **Seung-Hyun Woo**[4,‡], **Daniel D. Roybal**[5], **Gerard Karsenty**[6], **Ardem Patapoutian**[4,7], **David Sulzer**[3], and **Ellen A. Lumpkin**[1,2,8,¶]

[1]Dept of Physiology & Cellular Biophysics, Columbia University, New York, NY

[2]Program in Neurobiology & Behavior, Columbia University, New York, NY

[3]Depts of Psychiatry, Neurology and Pharmacology, Columbia University: Division of Molecular Therapeutics, New York State Psychiatric Institute, New York, NY

[4]The Scripps Research Institute, La Jolla, CA

[5]Pharmacology Graduate Program, Columbia University, New York, NY

[6]Department of Genetics and Development, Columbia University, New York, NY

[7]Howard Hughes Medical Institute

[8]Dept of Dermatology, Columbia University, New York, NY

[‡]Current Address: Genomics Institute of the Novartis Research Foundation, San Diego, CA

[¶]Lead Contact: Ellen A. Lumpkin, Ph.D., eal2166@columbia.edu

SUMMARY

Authors and Contributors
Conceptualization: BUH, EAL
Methodology: BUH, YB, TNG, EM, SW, AP, DZ, EAL
Software: BUH, YB
Formal Analysis: BUH, TNG, EAL
Investigation: BUH, YB, TNG, EM, SW, DR
Resources: GK
Data Curation: BUH, EAL
Writing- Original Draft: BUH, EAL
Writing-Review and Editing: BUH, SHW, TNG, EVM, GK, AP, DS, EAL
Visualization: BUH, TNG
Supervision: EAL
Project Administration: EAL
Funding Acquisition: BUH, EAL, AP

DECLARATIONS OF INTERESTS
The authors declare no competing interests.

Data and Software Availability
The RNA-seq data are accessible at Gene Expression Omnibus (GEO: GSE114336). Spike sorting and *ex vivo* data analysis software is freely available at www.github.com/buh2003/spikesortingPCA_DBSCAN. All other data are available from the authors upon request.

Epithelial-neuronal signaling is essential for sensory encoding in touch, itch and nociception; however, little is known about the release mechanisms and neurotransmitter receptors through which skin cells govern neuronal excitability. Merkel cells are mechanosensory epidermal cells that have long been proposed to activate neuronal afferents through chemical synaptic transmission. We employed a set of classical criteria for chemical neurotransmission as framework to test this hypothesis. RNA sequencing of adult mouse Merkel cells demonstrated that they express presynaptic molecules and biosynthetic machinery for adrenergic transmission. Moreover, live-cell imaging directly demonstrated that Merkel cells mediate activity- and VMAT-dependent release of fluorescent catecholamine neurotransmitter analogues. Touch-evoked firing in Merkel-cell afferents was inhibited either by pre-synaptic silencing of SNARE-mediated vesicle release from Merkel cells or by neuronal deletion of β_2-adrenergic receptors. Together, these results identify both pre- and postsynaptic mechanisms through which Merkel cells excite mechanosensory afferents to encode gentle touch.

Graphical Abstract

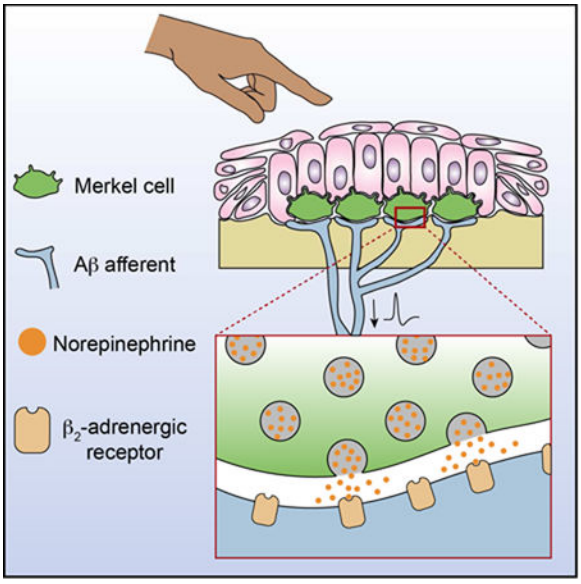

eTOC Blurb

Hoffman et al. reveal the molecular machinery underlying neurotransmission at a gentle-touch receptor. Employing Eccles' classical criteria for a chemical synapse, they show that epithelial Merkel cells communicate with sensory neurons through β2-adrenergic receptors at excitatory synapses.

INTRODUCTION

As a sensory-neural organ, skin provides both a protective barrier and an environmental interface that allows organisms to react to changing conditions. Signaling between epithelial cells and somatosensory neurons shape touch, itch, nociception and chemoreception (Wilson et al., 2013; Maksimovic et al., 2014; Baumbauer et al., 2015; Pang et al., 2015; Moehring et

al., 2018; Bellono et al., 2017). Little is known, however, about the mechanisms through which skin cells release neuroactive molecules to govern neuronal excitability.

Since their initial description as *"touch cells"*, Merkel cells have served as the archetypical skin cell that mediates somatosensation (Merkel, 1875). These epithelial derived cells complex with Aβ low-threshold mechanoreceptors (LTMRs) to produce slowly adapting type I (SAI) responses (Iggo and Muir, 1969; Woodbury and Koerber, 2007; Maricich et al., 2009; Morrison et al., 2009; Van Keymeulen et al., 2009). Recent work has demonstrated that Merkel cells mediate sustained SAI responses through Piezo2-dependent ion channels (Ikeda et al., 2014; Maksimovic et al., 2014; Woo et al., 2014). Moreover, optogenetics revealed that Merkel cells are necessary and sufficient to evoke sustained firing in Aβ LTMRs (Maksimovic et al., 2014). These studies establish Merkel cells as mechanosensory receptor cells, but the mechanisms through which these epidermal cells activate sensory neurons is still debated.

A longstanding model is that Merkel cells form chemical synapses with sensory afferents (Tachibana and Nawa, 2002; Maksimovic et al., 2013). Consistent with this hypothesis, Merkel cells are enriched in molecules that mediate synaptic vesicle release, and are immunoreactive for neurotransmitters, neuromodulators and neurotransmission machinery (Fantini and Johansson, 1995; Garcia-Caballero et al., 1989; Hartschuh and Weihe, 1988; Garcia-Caballero et al., 1989; Fantini and Johansson, 1995; Weihe et al., 1998; Leung and Wong, 2000; Haeberle et al., 2004; Tachibana and Nawa, 2005; Maksimovic et al., 2013). At the ultrastructural level, Merkel cells form synaptic-like contacts with sensory terminals; however, these are marked by dense-core vesicles rather than clear-core vesicles that typically mediate fast synaptic transmission (Andres, 1966; Breathnach and Robins, 1970; Chen et al., 1973; Mihara et al., 1979). Several studies have proposed the Merkel-cell neurite complex is either serotonergic or glutamatergic (Fagan and Cahusac, 2001; He et al., 2003; Hitchcock et al., 2004; Cahusac et al., 2005; Press et al., 2010; Chang et al., 2016). Nonetheless, direct functional evidence is lacking to identify the Merkel cell's presynaptic mechanisms and the neurotransmitter receptor(s) that act cell-autonomously in sensory neurons. Thus, we sought to systematically dissect molecular mechanisms that mediate neurotransmission at the Merkel cell-neurite complex.

As a framework for this analysis, we turned to the work of Eccles, who proposed a set of fundamental criteria for a *bona fide* chemical synapse based on Dale and Loewi's pioneering studies (Dale, 1937; Loewi, 1937; Eccles, 1964): 1) biosynthetic and degradative mechanisms for chemical transmission must be present in the presynaptic cell, 2) neurotransmitter must be present in the presynaptic cell, 3) neurotransmitter must be released when the presynaptic cell is stimulated, 4) the postsynaptic cell must be activated (or inactivated) by direct application of the neurotransmitter, and 5) pharmacological antagonism of the neurotransmitter must block the physiological action of the postsynaptic cell. By evaluating these classical criteria, we demonstrate that Merkel cells form SNARE-dependent chemical synapses that excite touch-sensitive neurons through adrenergic receptors.

RESULTS

Merkel cells are presynaptic, catecholaminergic cells

A handful of presynaptic proteins have been localized to Merkel cells; however, a genome-wide analysis of presynaptic signaling molecules in adult Merkel cells is lacking. We performed RNA sequencing (RNA-seq) on Merkel cells and keratinocytes purified from adult mice expressing an Atoh1-GFP fusion protein (*Atoh1*^{GFP}), which selectively marks Merkel cells in skin (Fig. 1A; Haeberle et al., 2004; Rose et al., 2009; Woo et al., 2014). RNA-seq analysis identified 3,364 genes that were differentially expressed between Merkel cells and basal keratinocytes (Fig. 1B, C; Table S1). Next, we generated a list of 542 genes encoding presynaptic molecules based on proteomic analyses of presynapses and gene ontology annotations (Table S2; Abul-Husn et al., 2009; Boyken et al., 2013; Aken et al., 2017; Blake et al., 2017). Of these, 123 genes were enriched in adult Merkel cells (Fig. 1D), in agreement with previous studies of neonatal Merkel cells (Haeberle et al., 2004). Merkel cell-enriched molecules span a wide range of presynaptic structures and functions, including the active zone, adhesion and cell surface, dense-core and synaptic vesicles, ion channels, transporters and receptors, neurotransmitter synthesis, and SNAREs. Thus, adult Merkel cells encode all the presynaptic machinery necessary for regulated release of neurotransmitters.

Dense-core vesicles package neuropeptides and small-molecule neurotransmitters such as monoamines, which are capable of exciting action potentials in neurons (Araneda and Firestein, 2006; Ramirez-Franco et al., 2016; Zhou et al., 2016). Monoamines include tryptophan-derived serotonin (5HT) and tyrosine-derived catecholamines, such as dopamine, epinephrine and norepinephrine. We noted that Merkel cells express *tyrosine hydroxylase* (*Th*), which encodes the rate-limiting enzyme in catecholamine synthesis (Fig 1D; Molinoff and Axelrod, 1971). To verify that Merkel cells express *Th*, we performed immunohistochemistry on full thickness skin specimens from *Th*^{GFP} reporter mice (Fig. 1E; Matsushita et al., 2002). Merkel cells and their Aβ LTMR afferents were identified by immunoreactivity to keratin 8 (K8) and neurofilament heavy chain (NFH), respectively (Vielkind et al., 1995; Maricich et al., 2009). Ninety-four percent of K8-positive Merkel cells expressed Th-GFP (n=406 Merkel cells from two mice). Merkel cells were also immunoreactive for TH protein (Fig. 1F). Along with *Th*, adult mouse Merkel cells express *Slc18a2* transcripts encoding VMAT2 (Table S2; 2.6±0.1; RPKM, mean±SEM, n=2 replicates), which preferentially loads catecholamines into synaptic vesicles, and *Maoa* transcripts (18.3±1.3), which encodes a key neuronal enzyme for monoamine degradation (Erickson et al., 1996; Shih et al., 1999). Thus, Merkel cells possess the machinery to synthesize catecholamines and load them into secretory vesicles.

Which catecholamines might Merkel cells synthesize? We performed high performance liquid chromatography (HPLC) coupled with electrochemical detection of monoamine neurotransmitters on whisker follicles, which are highly enriched in Merkel cells (Feigin et al., 2001; Larsen et al., 2002). Follicles were micro-dissected to reduce vascular contributions. To quantify the Merkel cell-dependent neurotransmitter content, we compared whisker follicles from adult *K14*^{Cre};*Atoh1*$^{LacZ/fl}$ mice, which lack Merkel cells, to littermate

controls, and found that norepinephrine was reduced by one-third in samples lacking Merkel cells (Fig. S1A–C). Given that whisker follicles are highly vascularized, sympathetic innervation is a likely source of residual norepinephrine in mice lacking Merkel cells. Epinephrine and 5HT were comparable between genotypes, and dopamine was not detected. The lack of dopamine suggests that dopamine is efficiently converted to norepinephrine in the follicle. Indeed, Merkel cells were immunoreactive for dopamine beta hydroxylase (DBH), which synthesizes norepinephrine from dopamine (Fig. S1D). These data suggest that epidermal Merkel cells are a significant source of norepinephrine but not 5HT, epinephrine or dopamine.

We were surprised to find that Merkel cells did not contribute to 5HT levels in whisker follicles, given that previous studies proposed that Merkel cells are serotonergic (He et al., 2003; Press et al., 2010; Chang et al., 2016; Chang et al., 2017). Consistent with our HPLC data, transcripts for the rate-limiting enzymes for 5HT bio-synthesis were not detected in adult mouse Merkel cells (*Tph1,* 0.13±0.02; *Tph2*, 0.01±0.01; RPKM, mean±SEM). Moreover, analysis of a transgenic GFP reporter strain for the ionotropic $5HT_{3A}$ receptor revealed that NFH^+ Aβ afferents that contacted mouse Merkel cells in touch domes and whisker follicles were not immunoreactive for $5HT_{3A}$-GFP (Fig. S1E; Gong et al., 2003). Instead, $5HT_{3A}$-GFP-expressing afferents lacked NFH immunoreactivity, indicating that they are unmyelinated C fibers or thinly myelinated Aδ fibers. These data are consistent with the role of $5HT_3$ in nociception (Zeitz et al., 2002; Kayser et al., 2007). Thus, we conclude that Merkel cell-neurite complexes in adult mice do not form $5HT_{3A}$-dependent serotonergic synapses.

In summary, these molecular and electrochemical results fulfill the first two of Eccles's criteria for a classical chemical synapse. Merkel cells express the biosynthetic and degradative machinery for adrenergic neurotransmitters. Moreover, the neurotransmitter norepinephrine in whisker follicles is dependent on Merkel cells. These results identify norepinephrine as a candidate neurotransmitter at Merkel cell-neurite complexes.

Merkel cells mediate uptake and touch-stimulated release of fluorescent neurotransmitters

We next asked whether Merkel cells package and release catecholamine neurotransmitters. We developed a semi-intact epidermal peel preparation that enables direct pharmacological and optical access to Merkel cells (Fig. S2A). *Atoh1* reporter mice expressing GFP were used to identify Merkel cells, which formed readily visualized clusters in touch domes (Lumpkin et al., 2003; Maricich et al., 2009; Rose et al., 2009). We confirmed that Merkel cells are excitable in this preparation by depolarizing with high-K^+ Ringer's solution or by delivering focal displacements during calcium imaging experiments (Haeberle et al., 2004; Ikeda et al., 2014; Maksimovic et al., 2014). Both stimuli elicited rapid, reversible and repeatable increases in cytoplasmic calcium (Fig. S2B–I; Videos S1, S2). Such calcium transients were abolished by antagonists of N- and P/Q-type (10 μM ω-conotoxin MVII-C) and L-type (10 μM nimodipine) voltage- gated Ca^{2+} channels (VGCCs; Fig. S2J–M), in agreement with studies of dissociated Merkel cells (Haeberle et al., 2004; Haeberle et al., 2008).

To visualize neurotransmitter packaging, we employed a VMAT2-selective, neurotransmitter analogue, fluorescent false neurotransmitter 206 (FFN206; Hu et al., 2013). Merkel cells reliably loaded FFN206 into puncta (328/330 Merkel cells from two animals) whereas surrounding keratinocytes showed no appreciable FFN206 accumulation. FFN206 puncta polarized to the cytoplasmic regions beneath nuclei (Fig. 2A; Video S3), recapitulating the distribution of dense-core vesicles and presynaptic proteins near neuronal contacts (Chen et al., 1973; Hartschuh and Weihe, 1980; Haeberle et al., 2004). Reserpine, a selective VMAT antagonist, abolished FFN206 fluorescence in Merkel cells, demonstrating that VMAT activity is required for FFN206 loading (Fig. 2B, C; Erickson et al., 1995). Thus, Merkel cells load VMAT2 substrates into subcellular puncta that likely represent secretory vesicle clusters.

To test whether Merkel cells are capable of evoked FFN206 release, we used live-cell imaging. Depolarization of FFN206-containing Merkel cells induced reliable destaining of FFN206 puncta (Fig. 2D–F), which was completely blocked by VGCC antagonists (Fig. 2G–I). Moreover, focal displacements caused rapid FFN206 destaining (Fig. 2J–L). Together, these data satisfy the functional release criterion of Eccles' classic chemical synapse: Merkel cells mediate evoked release of catecholaminergic vesicles in a VGCC-dependent manner.

Merkel cells employ SNARE-dependent vesicular release to mediate SAI responses

We next used a synaptic silencing approach to directly test whether Merkel cells employ vesicle fusion for neurotransmission. Adult Merkel cells are highly enriched in vesicle and target SNARE transcripts including vesicle associated membrane protein 2 (*Vamp2,* 331±51; RPKM, Fig. 1D). Tetanus neurotoxin light chain subunit (TeNT) cleaves VAMP2 to block vesicle fusion at synapses (Yamamoto et al., 2003; Yu et al., 2004; Zhang et al., 2008; Chandrashekar et al., 2009). We crossed $K14^{Cre}$ mice with $Rosa26^{floxstopTeNT\text{-}GFP}$ mice to selectively express TeNT in epidermal cells ($K14^{Cre};R26^{TeNT}$; Zhang et al., 2008; Morrison et al., 2009; Van Keymeulen et al., 2009). Control Merkel cells were enriched in VAMP2 protein compared with other epidermal cells (Fig. 3A). TeNT reduced the proportion of VAMP2-positive Merkel cells by threefold (Fig. 3A, B). Touch domes from $K14^{Cre};R26^{TeNT}$ mice showed innervated Merkel-cell clusters, suggesting that vesicular neurotransmitter release is not needed for the development and maintenance of Merkel-cell innervation (Fig. S3).

The functional consequences of epidermal-specific synaptic silencing were assessed with genotype-blind *ex vivo* single-unit recordings from Merkel-cell afferents, which were identified as fluorescently labeled, Aβ LTMR afferents that responded selectively to touch-dome indentation (Fig. S4A–C, Fig. 3C; Wellnitz et al., 2010). Littermate controls showed canonical SAI responses, characterized by high-frequency firing during dynamic stimulation and sustained low-frequency firing during static stimulation (Fig 3D). By contrast, Merkel-cell afferents from $K14^{Cre};R26^{TeNT}$ mice (Fig 3D) produced responses with a twofold reduction in dynamic firing, a threefold reduction in static firing rates, and intermediately adapting (IA) firing patterns (Fig. 3E, F). These responses phenocopied those from *Atoh1* conditional knockout mice, which completely lack Merkel cells, and epidermal-specific

Piezo2 knockout mice, which lack the Merkel cell's mechanotransduction channel (Maksimovic et al., 2014; Woo et al., 2014). Thus, SNARE-mediated vesicle release is required for the Merkel cell's contribution to SAI firing.

Norepinephrine evokes action potentials in Merkel-cell afferents

Eccles' fourth criterion is that the postsynaptic cell must be activated by direct application of the neurotransmitter. Norepinephrine, dopamine or 5HT was applied to receptive fields of Merkel-cell afferents during *ex vivo* skin-saphenous nerve recordings. Consistent with HPLC results, local application of norepinephrine evoke firing in Merkel-cell afferents in the absence of touch stimuli (Fig. 4A–C). By contrast, neither dopamine nor 5HT activated action potentials in these afferents. Moreover, norepinephrine did not activate firing in A-fiber rapidly adapting (RA) LTMRs (Fig. S5A, B). Thus, the excitatory effect of norepinephrine is not a general property of A-fiber LTMRs. Building on our Merkel-cell transcriptome analysis, which show that Merkel cells are equipped to synthesize norepinephrine, these results directly demonstrate that norepinephrine preferentially excites Merkel-cell afferents.

Neuronal β_2-adrenergic receptors mediate SAI responses

Norepinephrine signals through metabotropic adrenergic receptors (ARs; Hein and Kobilka, 1995). Qualitative immunohistochemistry showed co-localization of NFH and β_2AR immunoreactivity beneath some Merkel cells (Fig. 5A). Moreover, single-molecule *in situ* hybridization revealed that a subset of dorsal root ganglia (DRG) neurons marked by $TrkC^{tdTomato}$ and NFH, which includes Merkel-cell afferents, were enriched in β_2AR transcripts (*Adrb2;* Fig. S5C, D). Thus, β_2ARs are well positioned to mediate signaling downstream of norepinephrine release from Merkel cells.

To test if β_2ARs are required for touch-evoked SAI responses, we locally applied the selective β_2AR antagonist ICI 118,551 (henceforth referred to as ICI) to Merkel-cell afferents and delivered suprathreshold mechanical stimuli at 2-min intervals (Fig. 5B). Compared with vehicle-treated controls, ICI suppressed dynamic SAI firing by twofold and static firing by 3.5-fold (Fig. 5C–F). The effects of ICI on static SAI firing partially reversed within 60 min of ICI washout (Fig. S5E, F). Such incomplete washout from intact skin is not surprising, given the hydrophobic nature of ICI. Thus, touch-evoked SAI responses require activation of β_2ARs.

We then used a genetic approach to confirm that β_2ARs function cell-autonomously in neurons to mediate SAI responses. We made $Wnt1^{Cre};Adrb2^{fl/fl}$ mice, which harbor a deletion of β_2ARs in neural crest derivatives including somatosensory neurons (Jackson et al., 2012; Lewis et al., 2013). Touch domes from $Wnt1^{Cre};Adrb2^{fl/fl}$ and littermate control mice showed comparable Merkel cell-neurite complexes, indicating that touch-dome innervation is normal in neuronal β_2AR knockout mice (Fig. S5G, H). Compared with typical SAI responses in littermate controls, Merkel-cell afferents from $Wnt1^{Cre};Adrb2^{fl/fl}$ mice showed dramatically attenuated dynamic and static firing rates, and IA responses (Fig. 5G–J). Indeed, responses from $Wnt1^{Cre};Adrb2^{fl/fl}$ afferents were indistinguishable from those of *Atoh1* knockout mice lacking Merkel cells, mice whose Merkel cells lacked *Piezo2,*

and TeNT mice with synaptically silenced Merkel cells (Fig. 2; Fig S6). Together, these data demonstrate that neuronal β_2ARs are required for touch-evoked SAI responses (i.e. the physiological action of the post-synaptic cell), satisfying Eccles's fifth criterion.

DISCUSSION

Epithelial-neuronal crosstalk plays an essential role in sensory signaling; however, our understanding of release mechanisms and neurotransmitter receptors through which skin cells govern neuronal excitability is in its infancy. Adopting Eccles' definition of a *bona fide* chemical synapse, we demonstrate that epidermal Merkel cells excite the nervous system through SNARE-dependent adrenergic synapses. Our results show that Merkel cells express the biosynthetic and degradative machinery for adrenergic neurotransmission (criterion 1) and that norepinephrine in Merkel cell-rich skin areas depends on the presence of Merkel cells (criterion 2). In epidermis, Merkel cells selectively mediate VMAT- and VGCC-dependent evoked release of fluorescent catecholamines (criterion 3). Moreover, by using a tissue-specific genetic strategy to cleave Merkel-cell VAMP2, we directly demonstrate that SNARE-mediate vesicle release is essential for touch-evoked SAI responses. Turning to the postsynaptic cell, exogenous norepinephrine directly excites action potentials in Merkel-cell afferents (criterion 4), and touch-stimulated SAI responses are disrupted by pharmacological blockade or neuron-specific deletion of β_2ARs (criterion 5). Together, these results identify both pre- and postsynaptic mechanisms through which touch-dome Merkel cells excite mechanosensory afferents (Fig. 6).

The Merkel cell-neurite complex is an adrenergic synapse

Merkel cells are epithelial derived mechanosensory cells whose role in gentle touch has recently been clarified. Mice harboring an epidermal-specific deletion of the neuronal transcription factor *Atoh1* lack Merkel cells throughout the body (Maricich et al., 2009; Morrison et al., 2009; Van Keymeulen et al., 2009). Electrophysiological analysis of these mice showed that Merkel cells potentiate SAI firing rates during dynamic and static touch, and enable sustained firing during static pressure (Maksimovic et al., 2014). Moreover, sustained firing requires the mechanically gated ion channel Piezo2 in Merkel cells (Fig. S6; Ikeda et al., 2014; Maksimovic et al., 2014; Woo et al., 2014). Thus, Merkel cells enhance the excitability of Aβ LTMRs during dynamic touch stimuli and mediate mechanosensory responses to gentle pressure.

Merkel cells accomplish these functions by signaling to sensory neurons at adrenergic synapses. By silencing SNARE-mediated vesicle release in epidermis, we found that the responses of Merkel-cell afferents recapitulate the suppressed dynamic firing and truncated static firing observed in epidermal-specific *Atoh1* and *Piezo2* knockout mice (Maksimovic et al., 2014; Woo et al., 2014). These data are consistent with a recent report that bath-applied Botulinum toxin reduced compound action potentials in whisker afferents (Chang et al., 2016). Given that Merkel cells are highly enriched in VAMP2, the effects of epidermal TeNT expression are most likely due to VAMP2 cleavage in Merkel cells. Likewise, neuronal deletion of β2ARs phenocopied the effects of Merkel-cell synaptic silencing.

Together, these results suggest that SNARE-dependent neurotransmitter release followed by β2ARs activation on neurons accounts for the Merkel cell's role in SAI firing (Fig. 6).

This finding is surprising, given the plethora of candidate neuromodulators at the Merkel cell-neurite complex (Maksimovic et al., 2013). Neuropeptides such as CCK, VIP, Met-Enkephalin and substance P are present in Merkel cells (Hartschuh et al., 1979; Fantini and Johansson, 1995; Haeberle et al., 2004), and our transcriptome analysis demonstrates that the Merkel cells are fully equipped to release these peptides through dense-core vesicles. Neurotransmitters such as ATP and glutamate have also been proposed to mediate Merkel-cell signaling (Toyoshima and Shimamura, 1991; Nakamura and Strittmatter, 1996; Fagan and Cahusac, 2001; Haeberle et al., 2004; Hitchcock et al., 2004; Nunzi et al., 2004). As previous functional studies have used pharmacology in semi-intact preparations, it is unclear whether these transmitters mediate autocrine signaling in Merkel cells or paracrine signaling to other cell types in skin. Consistent with autocrine signaling, glutamate and ATP receptors are expressed in Merkel cells (Table S1; Haeberle et al., 2004). By contrast, we observed β2AR immunoreactivity at the terminals of Merkel-cell afferents, and neuronal deletion of β2AR indicates that adrenergic signaling acts intrinsically in neurons to enable SAI responses. Intriguingly, neuroanatomical studies suggest that Merkel cells are contacted by neurons other than Aβ SAI afferents, including thinly myelinated and unmyelinated fibers (Reinisch and Tschachler, 2005; Lesniak et al., 2014; Niu et al., 2014). Whether Merkel cells communicate with these fiber types through β2ARs or other signaling pathways is unknown.

5HT, which has well established roles in itch and nociception, has also been investigated in Merkel cells. Amperometry detected mechanically stimulated monoamine release from rodent whisker follicles (Chang et al., 2016); however, the methods employed do not distinguish 5HT from catecholamines (Pennington et al., 2004). Moreover, transcriptome analysis in this study indicates that adult mouse Merkel cells express the rate limiting enzyme for catecholamine synthesis but lack enzymes that produce 5HT. Moreover, 5HT did not excite action potentials in Merkel-cell afferents innervating touch domes, whereas norepinephrine elicited robust firing. These data stand in contrast with recent studies of 5HT signaling in mouse whisker afferents, which used suction electrode recordings of nerve bundles without spike sorting to isolate single-unit responses (Chang et al., 2016; Chang et al., 2017). Given 5HT receptors are broadly expressed among sensory neurons (Zeitz et al., 2002; Lin et al., 2011; Urtikova et al., 2012; Morita et al., 2015; Salzer et al., 2016), it is likely that many types of somatosensory neurons contribute to 5HT-evoked compound action potentials. Consistent with this interpretation, mouse whisker follicles receive abundant innervation by $5HT_{3A}$-positive, NFH-negative afferents, which are distinct from the NFH-positive Aβ LTMRs that innervate Merkel cells. Indeed, peripheral 5HT robustly excites NFH-negative sensory neurons that mediate itch and nociception (Hosogi et al., 2006; Rausl et al., 2013; Morita et al., 2015; Julius and Basbaum, 2001; Zeitz et al., 2002; Basbaum et al., 2009). Although our data do not support an excitatory role for 5HT signaling in mouse touch-dome afferents, Merkel cells might produce 5HT in other species or skin structures. An intriguing possibility is that Merkel cell-derived 5HT could potentiate NFH-negative sensory neurons in pathophysiological states such as chronic pain and itch. Indeed, a role for Merkel cells in mechanically evoked itch has been recently proposed (Feng et al., 2018).

Adrenergic signaling in the somatosensory system

Previous studies of adrenergic signaling in the somatosensory system have focused on nociception. In the descending antinociceptive system, for example, noradrenergic neurons in the locus coeruleus project to the dorsal horn of the spinal cord to inhibit nociceptive signals (Westlund and Coulter, 1980; Clark and Proudfit, 1991; Fields et al., 1991). In the periphery, the role of adrenergic signaling in nociception has been attributed to the sympathetic nervous system. After peripheral nerve injury or inflammation, sympathetic neurons sprout within DRG to sensitize nociceptive neurons to adrenergic stimulation (Sato and Perl, 1991; McLachlan et al., 1993; Bossut et al., 1996; Leem et al., 1997). Moreover, adrenergic compounds induces nociceptive responses in injured or inflamed skin (Chabal et al., 1992; Torebjörk et al., 1995; Choi and Rowbotham, 1997; Khasar et al., 1999). By contrast, norepinephrine does not elicit mechanonociceptive responses in naïve tissue (Fuchs et al., 2001). To our knowledge, adrenergic signaling has not been implicated in the encoding of gentle touch. Thus, our results define a previously unsuspected paradigm for adrenergic signaling in somatosensation.

β_2ARs and neuronal excitability

How might norepinephrine signaling through metabotropic β_2ARs excite action potentials in post-synaptic Aβ-LTMRs? A precedent for an excitatory metabotropic synapse is set by the retinal photoreceptor-ON bipolar cell synapse, which excites postsynaptic neurons via mGluR6 receptors coupled through $G\alpha_o$ signaling to TRPM1-dependent cation channels (Martemyanov and Sampath, 2017).

β_2ARs couple to $G\alpha_s$ signaling, which controls neuronal excitability through altering the activity of ion channels. $G\alpha_s$ activation stimulates adenylyl cyclase to increase adenosine 3', 5'-cyclic monophosphate (cAMP) and activate of downstream effectors such as cAMP-dependent protein kinase A (PKA; Rosenbaum et al., 2009), both of which can modulate ion channels. For example, in olfactory sensory neurons, a $G\alpha_{olf/s}$-coupled sensory transduction cascade culminates in gating of cyclic nucleotide gated (CNG) cation channels (Nakamura and Gold, 1987). CNG channels likewise function as a critical component of membrane depolarization in vertebrate phototransduction (Yau and Baylor, 1989) and underlie inward conductances and hippocampal neurons (Leinders-Zufall et al., 1995). Intriguingly, CNG channel expression is detected in NFH-positive DRG neurons (Usoskin et al., 2015). Intracellular cAMP also signals though hyperpolarization-activated cyclic nucleotide-gated (HCN) cation channels (Mayer and Westbrook, 1983). Currents mediated by HCN channels are found in many types of sensory neurons, including Aβ LTMRs (Gao et al., 2012; Chang et al., 2017). Finally, β_2ARs form a protein complex with $Ca_v1.2$ channels, which provides spatiotemporal coupling of β_2ARs to calcium channel activation (Davare et al., 2001). PKA mediated phosphorylation of $Ca_v1.2$ contributes to an increase in inward Ca^{2+} conductance (Hell et al., 1993; Gao et al., 1997; Bunemann et al., 1999). Such cAMP-PKA mediated modulation of ion channels can occur with a latency of 500 ms (Lancaster et al., 2006). Additionally, the compartmentalization of cAMP signals into microdomains by tonic phosphodiesterase activity has been proposed to enable local activation of cAMP-PKA signaling (Rich et al., 2000; Jurevicius et al., 2003). Together, these mechanisms suggest a plausible model of norepinephrine-evoked, β_2AR-mediated activation of Aβ LTMRs with

fast kinetics; however, future studies are needed to establish whether these signaling mechanisms mediate excitation in Merkel-cell afferents.

β_2-adrenergic signaling in health and disease

β-adrenergic signaling is a cornerstone therapeutic target for the treatment of cardiovascular diseases. β-blockers, which target β-adrenergic receptors, have been among the most widely used medicines for over half a century. A side effect of β-blocker therapy is paresthesia, or numbness and tingling (Van Buskirk, 1980; Stewart and Castelli, 1996). These symptoms are attributed to of the vascular effects of β-blockers in peripheral tissues; however, our findings suggest that paresthesia might be a result of β-blockers disrupting adrenergic signaling in sensory afferents.

STAR METHODS

Contact for reagent and resource sharing

Further information and requests for resources and reagents should be directed to Dr. Ellen A. Lumpkin (eal2166@columbia.edu).

Experimental Model and Subject Details

Animals—Animal use was conducted according to guidelines from the National Institutes of Health's Guide for the Care and Use of Laboratory Animals and was approved by the Institutional Animal Care and Use Committee of Columbia University Medical Center. Mice were maintained on a 12 h light/dark cycle, and food and water was provided *ad libitum.* All mice were healthy, and none of the experimental mice was immune compromised. Unless otherwise noted, mice of both sexes were used and mice were randomly allocated to experimental groups. The following strains were used in this study: $Atoh1^{GFP}$ (Rose et al., 2009), Th^{GFP} (Matsushita et al., 2002) which express GFP under the control of the *Th* promoter, wild-type (WT) C57BL/6J, $K14^{Cre}$ (Dassule et al., 2000), $Atoh1^{LacZ}$ (Ben-Arie et al., 2000), $Atoh1^{flox}$ (Shroyer et al., 2007), $5HT_{3A}$-EGFP (Gong et al., 2003), $Atoh1^{nGFP}$ (Lumpkin et al., 2003), $R26^{TeNT}$ (Zhang et al., 2008), $Wnt1^{Cre}$ (Lewis et al., 2013), $TrkC^{tdTomato}$ (Bai et al., 2015) and $B2AR^{flox}$ (Hinoi et al., 2008). *TeNT* mice were generated by crossing hemizygous $K14^{Cre}$ male with homozygous $R26^{TeNT}$ female mice. $Atoh1^{CKO}$ mice were generated as described previously (Morrison et al., 2009). Mice of the $K14^{Cre}$;$Atoh1^{LacZ/flox}$ genotype lacked expression of *Atoh1* in *K14*-expressing cells and were designated as $Atoh1^{CKO}$ mice. Genotypes that lacked either the Cre and/or LacZ alleles were designated as controls. $Ardb2^{CKO}$ mice were generated by first crossing hemizygous $Wnt1^{Cre}$ male with homozygous $Ardb2^{flox}$ mice. Male progeny hemizygous for $Wnt1^{Cre}$ and heterozygous for $Ardb2^{flox}$ ($Wnt1^{Cre}$;$Ardb2^{flox/+}$) were crossed with homozygous $Ardb2^{flox}$ female mice. Mice of the $Wnt1^{Cre}$;$Ardb2^{flox/flox}$ genotype were designated as experimental, and mice with the $Ardb2^{flox/flox}$ that lacked Cre were designated as controls. All mice were bred as recommended by The Jackson Laboratory. Genotyping was performed through a commercial service (Transnetyx).

Method Details

RNA sequencing and analysis

To isolate Merkel cells and keratinocytes for RNA-seq, dorsal skin from 7–8-week old female mice was removed and placed in a plastic dish, epidermis-side down. Skin was scraped with a scalpel to remove fat and muscle. Skin was then floated epidermis-side up in 0.25% trypsin for 2 h at 37°C. Epidermis was manually separated from the dermis, broken into smaller pieces, and recovered in culture media (CnT02, Chemicon) for 30 min with a stir bar. A 70-μm cell strainer was used to collect single cells. Cells were incubated with the Cd49f-PE antibody (BD Pharmingen) for 30 min on ice. GFP+/PE- Merkel cells and GFP-/PE+ keratinocytes were purified from the epidermal-cell suspension with FACS, directly into Trizol (ThermoFisher). Total RNA was isolated using commercially available reagents (Qiagen RNeasy kit) and DNAse-treated according to manufacturer's instructions to remove contaminating genomic DNA. First- and second-strand cDNA synthesis, and cDNA amplification was performed with the Ovation RNA-Seq System V2 (NuGEN). The cDNA library was prepared with the Ovation Ultralow System V2 (NuGEN). Sequencing was conducted on an Illumina HiSeq1000. Reads were aligned to the annotated mouse reference genome (mm10) with SAMtools (Li et al., 2009). Differential expression analysis was performed with DEseq2 (Love et al., 2014). The core presynaptic gene list (Table S2) was generated by combining published presynaptic proteomic libraries (Abul-Husn et al., 2009; Boyken et al., 2013) with the MGI (Blake et al., 2017) and Ensembl (Aken et al., 2017) presynapse (GO:0098793) gene ontology annotations (combined, 542 genes). Genes were manually annotated according to protein function using Gene Ontology annotations.

Semi-intact epidermal peel preparation

Live-cell imaging was performed in a semi-intact epidermal peel preparation. This preparation enables direct pharmacological and physiological access to Merkel cells *in situ.* Back skin from P20–24 *Atoh1*^{nGFP} or *Atoh1*^{GFP} mice was clipped with electric clippers, depilated (Surgi-cream), and dissected onto a small dish. Skin specimens (1 cm^2) were applied to glass coverslips epidermis-side down, in order to form a stable adhesion between the coverslip and epidermis. Samples were incubated in dispase (25 U/ml, Fisher Scientific) for 1 h at room temperature, on an orbital shaker. Using forceps, dermal and subcutaneous tissue was gently peeled from the epidermis, leaving only epidermal cells on the coverslip.

Immunohistochemistry

For cryosections, mouse skin was clipped with electric clippers, depilated (Surgi-cream) and dissected from the back (7–10-weeks of age). Tissue was fixed in 4% paraformaldehyde (PFA) for 30 min, cryoprotected in 30% sucrose overnight, frozen in OCT (Tissue-Tek), and sectioned at a thickness of 16–20 μm. For epidermal peel preparations, samples were fixed in 4% PFA for 30 min. Cryosectioned skin or epidermal peels were labeled at 4 overnight with the following primary antibodies: rat anti-K8 (TROMA1, Developmental Studies Hybridoma Bank, 1:100), chicken anti-NFH (Abcam: ab4680, 1:2,000), rabbit anti-VAMP2 (Abcam: ab3347, 1:500), rabbit anti-β2-AR (H-20, Santa Cruz: sc-569, 1:250), rabbit anti-TH (Millipore: AB152, 1:500), and rabbit anti-DBH (Immunostar: 22806, 1:2000). Secondary goat AlexaFluor-conjugated antibodies (Thermo Fisher Scientific) directed

against rat (Alexafluor 488, A-11006; Alexafluor 594, A-11007), chicken (Alexafluor 488, A-11039; Alexafluor 594, A-11042), or rabbit (Alexafluor 488, A-11008; Alexafluor 647, A-21450) IgG were used for 1 h at room temperature (1:1000). Samples were mounted with Fluoromount-G with DAPI (Thermo Fisher Scientific).

For whole-mount immunostaining with tissue clearing, skin was depilated, tape-stripped to remove the stratum corneum and dissected from the proximal hind limb of mice (7–10 weeks of age). For whisker whole-mount immunostaining, whiskers were isolated from whisker pads of mice (7–10 weeks of age), and whisker capsules were dissected to expose the ring sinus and external root sheath. Ring sinus was removed to expose the glassy membrane and Merkel cells within. Whole-mount immunohistochemistry was performed as previously described (Lesniak et al., 2014). Briefly, tissue was fixed in 4% PFA overnight, washed in 0.03% triton-X PBS (PBST) and incubated in primary antibody for 72–96 h at 4°C. Primary antibodies used were: rat anti-K8 (TROMA1, Developmental Studies Hybridoma Bank, 1:100), chicken anti-NFH (Abcam: ab4680, 1:500), rabbit anti-NFH (Abcam; ab8135, 1:500), and chicken anti-GFP (Abcam: ab13970, 1:500). After 5–10 h of washes in PBST, samples were incubated for 48 h at 4°C in secondary antibodies: goat AlexaFluor-conjug ated antibodies (Thermo Fisher Scientific) directed against rat (Alexafluor 488, A-11006; Alexafluor 647, A-21247), chicken (Alexafluor 488, A-11039; Alexafluor 594, A-11042) or rabbit (Alexafluor 594, A-11037) IgG. After staining, tissue was dehydrated progressively in 25%, 50%, 75% and 100% methanol in PBST (1 h each) and cleared using a 2:1 benzyl benzoate/benzyl alcohol solution.

Specimens were imaged in three dimensions (0.5–1 μm axial step sizes) on a Zeiss Exciter confocal microscope (LSM 5) equipped with 20X, 0.8 NA or 40X, 1.3 NA objective lenses.

In situ hybridization

DRG sections harvested from $TrkC^{tdTomato}$ mice (4 weeks of age) were cut at 25-μm thickness and processed for high-sensitivity RNA *in situ* detection using an RNAscope Fluorescent Detection Kit according to manufacturer's instructions (Advanced Cell Diagnostics, Hayward, California, USA). The following modifications were made to the protocol: after harvesting, DRG were fixed in 4% paraformaldehyde for 15 min and then incubated in 30% sucrose for 2 h at 4°C. Additional fixation steps were omitted from hybridization protocol. DRG were embedded in OCT (Sakura) and stored at −80°C until sectioned. Hybridization was performed using the *Adrb2 probe* (449771-C3, mouse), followed by incubation at 4°C overnight with rabbit anti-dsRed (1:3000, Clontech: 632496) and chicken anti-neurofilament heavy (1:5000, Abcam, ab4680) primary antibodies. Sections were then incubated at room temperature for 1 h with goat anti-rabbit AlexaFluor 594- (Thermo Fisher Scientific, A-11037) and anti-chicken AlexaFluor 647-conjugated (Thermo Fisher Scientific, A-21449) secondary antibodies. Samples were mounted with Fluoromount-G (Fisher Scientific). Specimens were imaged in three dimensions (1-μm axial steps) on a Nikon Ti Eclipse for scanning confocal microscopy equipped with a 40X, 1.3 NA objective lens. Images were analyzed using ImageJ software (Schneider et al., 2012). Quantification was performed on unprocessed axial stacks, following thresholding.

High performance liquid chromatography (HPLC)

Whisker pads were dissected from *Atoh1*^{CKO} and littermate control animals (7–10 weeks of age) and placed in a dissection dish with PBS. Samples were chilled on ice to prevent monoamine oxidation. Follicles were exposed in whisker pads for further micro-dissection. To reduce vascular contributions, follicles were trimmed at the junction between the ring and cavernous sinuses. Once trimmed, the ring sinus was removed to expose the glassy membrane and the Merkel cells within the external root sheath. Trimmed follicles were then separated from whisker pads by transection at the inner conical body. Micro-dissected follicles were immediately placed in a 0.1 M perchloric acid solution on ice. Four follicles were pooled per animal. Pooled follicles were homogenized with a hand held sonicator and centrifuged (15,000 rpm) at 4°C. Supernatant was then stored at −80°C or analyzed immediately. HPLC was performed as described previously (Feigin et al., 2001; Larsen et al., 2002). Briefly, HPLC coupled with electrochemical detection was performed on an ESA Coulochem II detector equipped with a model 5011 analytical cell (ESA) set at an applied potential of 400 mV and a Velosep RP-18 column (Applied Biosystems). The mobile phase contained 45 mM NaH_2PO_4, 0.2 mM EDTA, 1.2 mM heptanesulfonic acid and 5% methanol, adjusted to pH 3.2 with phosphoric acid. Total elution time was 30 min. Molar amounts of metabolites were calculated from areas under HPLC peaks using calibration curves and normalized to total sample weight.

FM1–43 injections

FM1–43 (Biotium; #70020) was used to visualize SAI receptive fields (touch domes) for electrophysiological recordings. FM1–43 was diluted at 1.5 mM in sterile PBS and injected subcutaneously (70 µl per mouse). Tissue was dissected for *ex vivo* skin–nerve electrophysiology 12–14 h after injection.

Ex vivo skin-nerve electrophysiology

Touch-evoked responses from cutaneous afferents were recorded after dissecting the hindlimb skin and saphenous nerve from 7–10 week old mice, according to published methods (Wellnitz et al., 2010). For identifying receptive fields, the skin was placed epidermis-side-up in a custom chamber and perfused with carbogen-buffered synthetic interstitial fluid (SIF) kept at 32 °C with a temperature controller (model TC-344B, Warner Instruments). The nerve was immersed in mineral oil in a recording chamber, teased apart with fine forceps, and small bundles were placed onto a silver recording electrode connected with a reference electrode to a differential amplifier (model 1800, A-M Systems). Conduction velocity was measured by electrically stimulating (Model 2100 isolated pulse stimulator, A-M Systems) receptive fields. Signals was band-passed filtered at 0.3–5 kHz, sampled at 20 kHz using a PowerLab 8/35 board (AD Instruments) and recorded using LabChart software (AD Instruments). SAI receptive fields (touch domes) labeled with FM1–43 were visualized using a fluorescence stereomicroscope equipped with a long-pass GFP filter set.

Spike sorting and data analysis was performed off-line with custom software in MATLAB (Hoffman and Lumpkin, 2018). Semi-unsupervised spike sorting was performed with principal component analysis (PCA) and density-based spatial clustering of applications

with noise (DBSCAN). Sorted spikes were then analyzed for metrics of spike timing, firing rate, and adaptation properties.

For these studies, we focused on Merkel-cell afferents in touch domes, as described by Iggo and Muir (Iggo and Muir, 1969). The afferents generally have no spontaneous firing, respond selectively to pressure applied directly to a touch dome, and are particularly sensitive to moving stimuli but are insensitive to hair tugging and skin stretch (Iggo and Muir, 1969). To identify responses from these afferents in mutant and control genotypes, we used a mechanical search paradigm with a fine glass probe. Afferents were classified as 'Merkel-cell afferents' according to the following criteria: (1) Aβ conduction velocity (≥ 9 m s^{-1}), (2) punctate receptive fields restricted to one or more fluorescently labeled touch domes, (3) insensitive to pressure applied to skin areas adjacent to touch domes, (4) insensitive to hair tugging but responsive when the hair is bent to compress the touch dome. Touch-sensitive afferents that did not meet these criteria were not analyzed further. Fibers were classified as SA if spikes were observed during the last 1 s of the hold phase of stimulation in ≥75% of stimulus presentations, otherwise they were classified as IA. Recordings and analyses of $K14^{Cre};R26^{TeNT}$, $Wnt1^{Cre};Adrb2^{fl/fl}$, and their controls were performed blind to genotype (Table S3).

Afferents were classified as A-fiber RA-LTMRs according to the following criteria: (1) A-fiber conduction velocity (>1 m s^{-1}), (2) rapid adaptation to mechanical indentation, (3) sensitive to low-force stimulation with von Frey monofilaments (<0.4 mN).

Mechanical responses were elicited with von Frey monofilaments and a custom-built mechanical stimulator. The automated mechanical stimulator applied stimuli with an indenter (tip diameter, 1.6 mm), and stimuli were commanded using a model XPS motion controller and driver system (Newport) connected to a PC computer. Movement of the indenter was controlled with custom software and measured with a laser distance-measuring device (OptipNCDT 1402, Micro-Epsilon). Touch stimuli consisted of ramp and 5-s hold indentations. First-order approximation of approach speed was 3.2 mm s^{-1}. The mechanical stimulator tip was held ~600 μm from the surface of the skin. Mechanical displacements ranged from the point of skin contact to 450 μm of skin indentation. For non-pharmacological experiments, the period between successive displacements was 60 s. For pharmacological experiments, the period between successive displacements was 120 s.

For pharmacology, receptive fields, conduction velocity and von Frey thresholds were first identified with the epidermis-side facing up. After identification of a Merkel-cell afferent based on FM1–43 fluorescence and the SAI response pattern, the skin was inverted such that the dermis side faced up for perfusion. Receptive fields were then isolated with a custom-built glass perfusion ring. For experiments performed in the absence of mechanical stimulation, drugs were directly applied to the isolated receptive fields (Norepinephrine, Tocris, 5169; Serotonin, Tocris, 3547; Dopamine, Sigma Aldrich, H8502) and evoked responses were recorded in gap-free mode. For experiments performed with simultaneous pharmacological application and mechanical stimulation, both drugs and mechanical indentation were applied to receptive fields within the perfusion ring (ICI 118,551, Tocris, 0821). To accommodate for repeated mechanical stimulations over long periods of time, we

reduced the magnitude of mechanical stimuli for pharmacological experiments. Thus, recorded firing rates from pharmacological experiments were slightly lower than in non-pharmacological experiments (compare Fig. 3D-F to Fig. 5B-F).

Norepinephrine-response data were fit with the following four-parameter logistic equation:

$$y = \frac{a - b}{1 + 10^{(((\log_{10} c) - x) \times d)}} + b$$

a = maximum; b = minimum; $c = EC_{50}$; d = Hill's slope

Calcium imaging

Semi-intact epidermal peel preparations were isolated from *Atoh1*^{nGFP} or *Atoh1*^{GFP} mice. Merkel cells were loaded for 30 mins at 37°C with 5 μM fura-2 acetoxymethyl ester (Thermo Fisher Scientific) and 1 μM pluronic acid (Pluronic F-127, Thermo Fisher Scientific) in a modified Ringer's solution (in mM): 140 NaCl, 5 KCl, 10 HEPES (pH 7.4), 10 D-Glucose, 2 $MgCl_2$, and 2 $CaCl_2$ (osmolality: 290 mmolkg^{-1}). Cells were given 30 min in Ringers solution to digest the ester bonds before imaging. Merkel cells were depolarized with mechanical stimulation or with high potassium extracellular solution (in mM): 5 NaCl, 140 KCl, 10 HEPES (pH 7.4), 10 D-Glucose, 2 $MgCl_2$, and 2 $CaCl_2$ (osmolality: 290 mmolkg^{-1}). Mechanical stimulation was delivered with a glass probe (tip diameter: ~0.5 μm) driven with a stepper motor (model MP-200, Sutter Instruments). The glass probe was positioned at an angle of 40° to the coverslip. To ensure that mechanosensitive channels were not activated at rest, displacements began from an offset position located 2–3 μm away from Merkel cells (Drew et al., 2002). For experiments with voltage-gated calcium channel blockers (nimodipine, Tocris, 0600; ω-Conotoxin MVIIC, Sigma Aldrich, C4188), Merkel cells were incubated with blockers for 30 min before imaging. Data were acquired with Metafluor software (version 7.6.3, Molecular Devices), and analyzed with ImageJ. Briefly, xy shifts were corrected in 340-nm and 380-nm images using a rigid body transformation with the "StackReg" plugin (Plugins/Registration/StackReg/RigidBody). Images of the fluorescence ratio at 340 nm and 380 nm excitation ($F_{340/380}$) were created with the "Image Calculator" (Image/Image Calculator). Regions of interest (ROIs) were drawn based on identified Merkel cells. Mean ROI fluorescence intensity over time was quantified with the "Time Series Analyzer V3" (Plugins/Time Series Analyzer V3). $\Delta F/F$ values were calculated as follows: $(F\text{-}F_i)/F_i$, where F is the $F_{340/380}$ at each frame and F_i is the average $F_{340/380}$ for the 30-s prior to stimulation. Samples were imaged with a 20x, 0.95 NA objective lens.

FFN imaging

Semi-intact epidermal peel preparations were isolated from *Atoh1*^{nGFP} or *Atoh1*^{GFP} mice. Merkel cells were loaded for 30 minutes at 37°C with 1 μM FFN206 (Tocris) in a modified Ringer's solution (in mM): 140 NaCl, 5 KCl, 10 HEPES (pH 7.4), 10 D-Glucose, 2 $MgCl_2$, and 2 $CaCl_2$ (osmolality: 290 mmolkg^{-1}). Merkel cells were depolarized with mechanical stimulation or with high potassium extracellular solution (in mM): 5 NaCl, 140 KCl, 10 HEPES (pH 7.4), 10 D-Glucose, 2 $MgCl_2$, and 2 $CaCl_2$ (osmolality: 290 mmolkg^{-1}). Mechanical stimulation was delivered with a glass probe (tip diameter: ~0.5 μm) driven by a

piezoelectric actuator (model PA8/12, Piezosystem Jeno; power supply ENV40 C, Piezosystem Jena). The glass probe was positioned at an angle of 40° to the coverslip. Displacements were triggered by a pClamp-controlled command voltage passed to the actuator driver through a low-pass filter (f_{cutoff}: 500 Hz; model LPF-100A, Warner Instruments). Displacement magnitudes were visually calibrated daily. To ensure that mechanosensitive channels were not activated at rest, displacements began from an offset position located 2–3 μm away from Merkel cells (Drew et al., 2002). For experiments with voltage-gated calcium channel blockers (nimodipine, Tocris, 0600; ω-Conotoxin MVIIC, Sigma Aldrich, C4188), Merkel cells were incubated with blockers for 30 minutes before imaging. Data were acquired with Metafluor software (version 7.6.3, Molecular Devices).

ImageJ and Matlab were used to analyze FFN206 destaining experiments. First, xy shifts were corrected in ImageJ using a rigid body transformation with the "StackReg" plugin (Plugins/Registration/StackReg/RigidBody). Next, regions of interest (ROIs) were drawn based on FFN206 puncta within GFP-positive Merkel cells. Mean ROI fluorescence intensity over time was quantified with the "Time Series Analyzer V3" (Plugins/Time Series Analyzer V3). All further analyses were performed in Matlab. To correct for bleaching, the baseline intensity values for each ROI were individually fit with a monoexponential decay function. To obtain bleaching-corrected values, fluorescence values (F) were subtracted from the monoexponential fit (F_{exp}) for that ROI ($F_{corr}=1+F-F_{exp}$). Baseline normalized values (F/F_i) were calculated by dividing bleaching-corrected fluorescence values (F) for each time point by the mean of the first 30 sec of each ROI (F_i). Puncta were classified as "destaining" if they exhibited at least 2% decrease in (F/F_i) 240 s after high-K^+ stimulation or 40 s after mechanical stimulation. Samples were imaged with a 20x, 0.95 NA objective lens (Olympus).

Quantification and Statistical Analysis

Analysis was performed in R (R-Project; R Development Core Team, 2010), Matlab (MathWorks), and Prism (Graphpad). Detailed statistical parameters are described in figure legends. Data are represented as mean±SEM and *n* represents the number of cells or independent experiments. For parametric data with three or more groups, one-way or two-way ANOVAs were followed by *post hoc* analyses for between-group comparisons. Unpaired, non-parametric data were analyzed using the Kruskal-Wallis test with Dunn's *post hoc* comparison. Paired data were compared with a matched two-way ANOVA with Sidak's *post hoc.* Student's two-tailed *t* test was used to compare means of two normally distributed groups. Categorical data were compared using the two-tailed Fisher's exact test. The normality of population data was assessed using the Kolmogorov-Smirnov test with Dallal-Wilkinson-Lilliefors P values, with $P<0.05$ indicating non-normality. Data were considered significant if $P<0.05$. Statistical details of experiments can be found in figure legends.

Supplementary Material

Refer to Web version on PubMed Central for supplementary material.

ACKNOWLEDGMENTS

Thanks to Drs. Eric Larson, Sue Kinnamon, Tom Finger and Charles Zuker for advice and reagents, Dr. Joriene de Nooij for sharing neuronal gene expression data prior to publication, Mr. Adan Horta for advice on transcriptome analysis, and members of the Lumpkin laboratory for discussions and comments on the manuscript. This research was supported by NIAMS (R01AR051219, EAL) and NINDS (F31NS105449, BUH). Authors are funded by the NIH (R01NS095435, R01MH108186, R01DA07418 DS), Burroughs Wellcome Fund PDEP program (TNG), NIGMS (T32GM007367, BUH), JPB Foundation (DS) and the Howard Hughes Medical Institute (AP). RNAseq was performed with support from the Genomics Institute of the Novartis Research Foundation. Core facilities were supported by NIAMS P30AR044535 and NCI P30CA013696. Funders had no role in study design, data collection and interpretation, or the decision to submit the work for publication.

REFERENCES

Abul-Husn NS, Bushlin I, Moron JA, Jenkins SL, Dolios G, Wang R, Iyengar R, Ma'ayan A, and Devi LA (2009). Systems approach to explore components and interactions in the presynapse. Proteomics 9, 3303–3315. [PubMed: 19562802]

Aken BL, Achuthan P, Akanni W, Amode MR, Bernsdorff F, Bhai J, Billis K, Carvalho-Silva D, Cummins C, Clapham P, et al. (2017). Ensembl 2017. Nucleic Acids Res 45, D635–d642. [PubMed: 27899575]

Andres KH (1966). [On the fine structure of Merkel's tactile apparatus in the sinus hair]. Naturwissenschaften 53, 706.

Araneda RC, and Firestein S (2006). Adrenergic enhancement of inhibitory transmission in the accessory olfactory bulb. J Neurosci 26, 3292–3298. [PubMed: 16554479]

Bai L, Lehnert BP, Liu J, Neubarth NL, Dickendesher TL, Nwe PH, Cassidy C, Woodbury CJ, and Ginty DD (2015). Genetic Identification of an Expansive Mechanoreceptor Sensitive to Skin Stroking. Cell 163, 1783–1795. [PubMed: 26687362]

Basbaum AI, Bautista DM, Scherrer G, and Julius D (2009). Cellular and molecular mechanisms of pain. Cell 139, 267–284. [PubMed: 19837031]

Baumbauer KM, DeBerry JJ, Adelman PC, Miller RH, Hachisuka J, Lee KH, Ross SE, Koerber HR, Davis BM, and Albers KM (2015). Keratinocytes can modulate and directly initiate nociceptive responses. Elife 4.

Bellono NW, Bayrer JR, Leitch DB, Castro J, Zhang C, O'Donnell TA, Brierley SM, Ingraham HA, and Julius D (2017). Enterochromaffin Cells Are Gut Chemosensors that Couple to Sensory Neural Pathways. Cell 170, 185–198.e116. [PubMed: 28648659]

Ben-Arie N, Hassan BA, Bermingham NA, Malicki DM, Armstrong D, Matzuk M, Bellen HJ, and Zoghbi HY (2000). Functional conservation of atonal and Math1 in the CNS and PNS. Development 127, 1039–1048. [PubMed: 10662643]

Blake JA, Eppig JT, Kadin JA, Richardson JE, Smith CL, and Bult CJ (2017). Mouse Genome Database (MGD)-2017: community knowledge resource for the laboratory mouse. Nucleic Acids Res 45, D723–d729. [PubMed: 27899570]

Bossut DF, Shea VK, and Perl ER (1996). Sympathectomy induces adrenergic excitability of cutaneous C-fiber nociceptors. J Neurophysiol 75, 514–517. [PubMed: 8822575]

Boyken J, Gronborg M, Riedel D, Urlaub H, Jahn R, and Chua JJ (2013). Molecular profiling of synaptic vesicle docking sites reveals novel proteins but few differences between glutamatergic and GABAergic synapses. Neuron 78, 285–297. [PubMed: 23622064]

Breathnach AS, and Robins J (1970). Ultrastructural observations on Merkel cells in human foetal skin. J Anat 106, 411.

Bunemann M, Gerhardstein BL, Gao T, and Hosey MM (1999). Functional regulation of L-type calcium channels via protein kinase A-mediated phosphorylation of the beta(2) subunit. J Biol Chem 274, 33851–33854. [PubMed: 10567342]

Cahusac PM, Senok SS, Hitchcock IS, Genever PG, and Baumann KI (2005). Are unconventional NMDA receptors involved in slowly adapting type I mechanoreceptor responses? Neuroscience 133, 763–773. [PubMed: 15908129]

Chabal C, Jacobson L, Russell LC, and Burchiel KJ (1992). Pain response to perineuromal injection of normal saline, epinephrine, and lidocaine in humans. Pain 49, 9–12. [PubMed: 1594285]

Chandrashekar J, Yarmolinsky D, von Buchholtz L, Oka Y, Sly W, Ryba NJ, and Zuker CS (2009). The taste of carbonation. Science 326, 443–445. [PubMed: 19833970]

Chang W, Kanda H, Ikeda R, Ling J, DeBerry JJ, and Gu JG (2016). Merkel disc is a serotonergic synapse in the epidermis for transmitting tactile signals in mammals. Proc Natl Acad Sci U S A 113, E5491–5500. [PubMed: 27573850]

Chang W, Kanda H, Ikeda R, Ling J, and Gu JG (2017). Serotonergic transmission at Merkel discs: modulation by exogenously applied chemical messengers and involvement of Ih currents. J Neurochem 141, 565–576. [PubMed: 28267198]

Chen SY, Gerson S, and Meyer J (1973). The fusion of Merkel cell granules with a synapse-like structure. J Invest Dermatol 61, 290–292. [PubMed: 4749462]

Choi B, and Rowbotham MC (1997). Effect of adrenergic receptor activation on post-herpetic neuralgia pain and sensory disturbances. Pain 69, 55–63. [PubMed: 9060013]

Clark FM, and Proudfit HK (1991). The projection of locus coeruleus neurons to the spinal cord in the rat determined by anterograde tracing combined with immunocytochemistry. Brain Res 538, 231–245. [PubMed: 2012966]

Dale H (1937). Some recent extensions of the chemical transmission of the effects of nerve impulses. In Les Prix Nobel en 1936 (Stockholm: Imprimerie Royale P.A. Norstedt & Söner), pp. 1–12.

Dassule HR, Lewis P, Bei M, Maas R, and McMahon AP (2000). Sonic hedgehog regulates growth and morphogenesis of the tooth. Development 127, 4775–4785. [PubMed: 11044393]

Davare MA, Avdonin V, Hall DD, Peden EM, Burette A, Weinberg RJ, Horne MC, Hoshi T, and Hell JW (2001). A beta2 adrenergic receptor signaling complex assembled with the Ca2+ channel Cav1.2. Science 293, 98–101. [PubMed: 11441182]

Drew LJ, Wood JN, and Cesare P (2002). Distinct mechanosensitive properties of capsaicin-sensitive and -insensitive sensory neurons. J Neurosci 22, RC228. [PubMed: 12045233]

Eccles JC (1964). The physiology of synapses (New York: Academic Press Inc., Publishers).

Erickson JD, Eiden LE, Schafer MK, and Weihe E (1995). Reserpine- and tetrabenazine-sensitive transport of (3)H-histamine by the neuronal isoform of the vesicular monoamine transporter. J Mol Neurosci 6, 277–287. [PubMed: 8860238]

Erickson JD, Schafer MK, Bonner TI, Eiden LE, and Weihe E (1996). Distinct pharmacological properties and distribution in neurons and endocrine cells of two isoforms of the human vesicular monoamine transporter. Proc Natl Acad Sci U S A 93, 5166–5171. [PubMed: 8643547]

Fagan BM, and Cahusac PM (2001). Evidence for glutamate receptor mediated transmission at mechanoreceptors in the skin. Neuroreport 12, 341–347. [PubMed: 11209947]

Fantini F, and Johansson O (1995). Neurochemical markers in human cutaneous Merkel cells. An immunohistochemical investigation. Exp Dermatol 4, 365–371. [PubMed: 8608344]

Feigin A, Fukuda M, Dhawan V, Przedborski S, Jackson-Lewis V, Mentis MJ, Moeller JR, and Eidelberg D (2001). Metabolic correlates of levodopa response in Parkinson's disease. Neurology 57, 2083–2088. [PubMed: 11739830]

Feng J, Luo J, Yang P, Du J, Kim BS, and Hu H (2018). Piezo2 channel-Merkel cell signaling modulates the conversion of touch to itch. Science 360, 530–533. [PubMed: 29724954]

Fields HL, Heinricher MM, and Mason P (1991). Neurotransmitters in nociceptive modulatory circuits. Annu Rev Neurosci 14, 219–245. [PubMed: 1674413]

Fuchs PN, Meyer RA, and Raja SN (2001). Heat, but not mechanical hyperalgesia, following adrenergic injections in normal human skin. Pain 90, 15–23. [PubMed: 11166966]

Gao LL, McMullan S, Djouhri L, Acosta C, Harper AA, and Lawson SN (2012). Expression and properties of hyperpolarization-activated current in rat dorsal root ganglion neurons with known sensory function. J Physiol 590, 4691–4705. [PubMed: 22753545]

Gao T, Yatani A, Dell'Acqua ML, Sako H, Green SA, Dascal N, Scott JD, and Hosey MM (1997). cAMP-dependent regulation of cardiac L-type Ca2+ channels requires membrane targeting of PKA and phosphorylation of channel subunits. Neuron 19, 185–196. [PubMed: 9247274]

Garcia-Caballero T, Gallego R, Roson E, Basanta D, Morel G, and Beiras A (1989). Localization of serotonin-like immunoreactivity in the Merkel cells of pig snout skin. Anat Rec 225, 267–271. [PubMed: 2589641]

Gong S, Zheng C, Doughty ML, Losos K, Didkovsky N, Schambra UB, Nowak NJ, Joyner A, Leblanc G, Hatten ME, et al. (2003). A gene expression atlas of the central nervous system based on bacterial artificial chromosomes. Nature 425, 917–925. [PubMed: 14586460]

Haeberle H, Bryan LA, Vadakkan TJ, Dickinson ME, and Lumpkin EA (2008). Swelling-activated Ca2+ channels trigger Ca2+ signals in Merkel cells. PLoS One 3, e1750. [PubMed: 18454189]

Haeberle H, Fujiwara M, Chuang J, Medina MM, Panditrao MV, Bechstedt S, Howard J, and Lumpkin EA (2004). Molecular profiling reveals synaptic release machinery in Merkel cells. Proc Natl Acad Sci U S A 101, 14503–14508. [PubMed: 15448211]

Hartschuh W, and Weihe E (1980). Fine structural analysis of the synaptic junction of Merkel cell-axon-complexes. J Invest Dermatol 75, 159–165. [PubMed: 6774030]

Hartschuh W, and Weihe E (1988). Multiple messenger candidates and marker substance in the mammalian Merkel cell-axon complex: a light and electron microscopic immunohistochemical study. Prog Brain Res 74, 181–187. [PubMed: 3187030]

Hartschuh W, Weihe E, Buchler M, Helmstaedter V, Feurle GE, and Forssmann WG (1979). Met enkephalin-like immunoreactivity in Merkel cells. Cell Tissue Res 201, 343–348. [PubMed: 509486]

He L, Tuckett RP, and English KB (2003). 5-HT2 and 3 receptor antagonists suppress the response of rat type I slowly adapting mechanoreceptor: an in vitro study. Brain Res 969, 230–236. [PubMed: 12676383]

Hein L, and Kobilka BK (1995). Adrenergic receptor signal transduction and regulation. Neuropharmacology 34, 357–366. [PubMed: 7566466]

Hell JW, Yokoyama CT, Wong ST, Warner C, Snutch TP, and Catterall WA (1993). Differential phosphorylation of two size forms of the neuronal class C L-type calcium channel alpha 1 subunit. J Biol Chem 268, 19451–19457. [PubMed: 8396138]

Hinoi E, Gao N, Jung DY, Yadav V, Yoshizawa T, Myers MG, Jr., Chua SC, Jr., Kim JK, Kaestner KH, and Karsenty G (2008). The sympathetic tone mediates leptin's inhibition of insulin secretion by modulating osteocalcin bioactivity. J Cell Biol 183, 1235–1242. [PubMed: 19103808]

Hitchcock IS, Genever PG, and Cahusac PM (2004). Essential components for a glutamatergic synapse between Merkel cell and nerve terminal in rats. Neurosci Lett 362, 196–199. [PubMed: 15158013]

Hoffman BU, and Lumpkin EA (2018). buh2003/SpikeSortingPCA_DBSCAN: SpikeSortingPCA_DBSCAN v1.0.1 (Version v1.0.01). Zenodo.

Hosogi M, Schmelz M, Miyachi Y, and Ikoma A (2006). Bradykinin is a potent pruritogen in atopic dermatitis: a switch from pain to itch. Pain 126, 16–23. [PubMed: 16842920]

Hu G, Henke A, Karpowicz RJ, Jr., Sonders MS, Farrimond F, Edwards R, Sulzer D, and Sames D (2013). New fluorescent substrate enables quantitative and high-throughput examination of vesicular monoamine transporter 2 (VMAT2). ACS Chem Biol 8, 1947–1954. [PubMed: 23859623]

Iggo A, and Muir AR (1969). The structure and function of a slowly adapting touch corpuscle in hairy skin. J Physiol 200, 763–796. [PubMed: 4974746]

Ikeda R, Cha M, Ling J, Jia Z, Coyle D, and Gu JG (2014). Merkel cells transduce and encode tactile stimuli to drive Abeta-afferent impulses. Cell 157, 664–675. [PubMed: 24746027]

Jackson CR, Ruan GX, Aseem F, Abey J, Gamble K, Stanwood G, Palmiter RD, Iuvone PM, and McMahon DG (2012). Retinal dopamine mediates multiple dimensions of light-adapted vision. J Neurosci 32, 9359–9368. [PubMed: 22764243]

Julius D, and Basbaum AI (2001). Molecular mechanisms of nociception. Nature 413, 203–210. [PubMed: 11557989]

Jurevicius J, Skeberdis VA, and Fischmeister R (2003). Role of cyclic nucleotide phosphodiesterase isoforms in cAMP compartmentation following beta2-adrenergic stimulation of ICa,L in frog ventricular myocytes. J Physiol 551, 239–252. [PubMed: 12815180]

Kayser V, Elfassi IE, Aubel B, Melfort M, Julius D, Gingrich JA, Hamon M, and Bourgoin S (2007). Mechanical, thermal and formalin-induced nociception is differentially altered in 5-HT1A−/−, 5-

HT1B−/−, 5-HT2A−/−, 5-HT3A−/− and 5-HTT−/− knock-out male mice. Pain 130, 235–248. [PubMed: 17250964]

Khasar SG, McCarter G, and Levine JD (1999). Epinephrine produces a beta-adrenergic receptor-mediated mechanical hyperalgesia and in vitro sensitization of rat nociceptors. J Neurophysiol 81, 1104–1112. [PubMed: 10085337]

Lancaster B, Hu H, Gibb B, and Storm JF (2006). Kinetics of ion channel modulation by cAMP in rat hippocampal neurones. J Physiol 576, 403–417. [PubMed: 16901946]

Larsen KE, Fon EA, Hastings TG, Edwards RH, and Sulzer D (2002). Methamphetamine-induced degeneration of dopaminergic neurons involves autophagy and upregulation of dopamine synthesis. J Neurosci 22, 8951–8960. [PubMed: 12388602]

Leem JW, Gwak YS, Nam TS, and Paik KS (1997). Involvement of alpha2-adrenoceptors in mediating sympathetic excitation of injured dorsal root ganglion neurons in rats with spinal nerve ligation. Neurosci Lett 234, 39–42. [PubMed: 9347941]

Leinders-Zufall T, Rosenboom H, Barnstable CJ, Shepherd GM, and Zufall F (1995). A calcium-permeable cGMP-activated cation conductance in hippocampal neurons. Neuroreport 6, 1761–1765. [PubMed: 8541476]

Lesniak DR, Marshall KL, Wellnitz SA, Jenkins BA, Baba Y, Rasband MN, Gerling GJ, and Lumpkin EA (2014). Computation identifies structural features that govern neuronal firing properties in slowly adapting touch receptors. Elife 3, e01488. [PubMed: 24448409]

Leung MS, and Wong CC (2000). Expressions of putative neurotransmitters and neuronal growth related genes in Merkel cell-neurite complexes of the rats. Life Sci 66, 1481–1490. [PubMed: 10794495]

Lewis AE, Vasudevan HN, O'Neill AK, Soriano P, and Bush JO (2013). The widely used Wnt1-Cre transgene causes developmental phenotypes by ectopic activation of Wnt signaling. Dev Biol 379, 229–234. [PubMed: 23648512]

Li H, Handsaker B, Wysoker A, Fennell T, Ruan J, Homer N, Marth G, Abecasis G, and Durbin R (2009). The Sequence Alignment/Map format and SAMtools. Bioinformatics 25, 2078–2079. [PubMed: 19505943]

Lin SY, Chang WJ, Lin CS, Huang CY, Wang HF, and Sun WH (2011). Serotonin receptor 5-HT2B mediates serotonin-induced mechanical hyperalgesia. J Neurosci 31, 1410–1418. [PubMed: 21273425]

Loewi O (1937). Die chemische übertragung der nervenwirkung. In Les Prix Nobel en 1936 (Stockholm: Imprimerie Royale P.A. Norstedt & Söner), pp. 1–14.

Love MI, Huber W, and Anders S (2014). Moderated estimation of fold change and dispersion for RNA-seq data with DESeq2. Genome Biol 15, 550. [PubMed: 25516281]

Lumpkin EA, Collisson T, Parab P, Omer-Abdalla A, Haeberle H, Chen P, Doetzlhofer A, White P, Groves A, Segil N, et al. (2003). Math1-driven GFP expression in the developing nervous system of transgenic mice. Gene Expr Patterns 3, 389–395. [PubMed: 12915300]

Maksimovic S, Baba Y, and Lumpkin EA (2013). Neurotransmitters and synaptic components in the Merkel cell-neurite complex, a gentle-touch receptor. Ann N Y Acad Sci 1279, 13–21. [PubMed: 23530998]

Maksimovic S, Nakatani M, Baba Y, Nelson AM, Marshall KL, Wellnitz SA, Firozi P, Woo SH, Ranade S, Patapoutian A, et al. (2014). Epidermal Merkel cells are mechanosensory cells that tune mammalian touch receptors. Nature 509, 617–621. [PubMed: 24717432]

Maricich SM, Wellnitz SA, Nelson AM, Lesniak DR, Gerling GJ, Lumpkin EA, and Zoghbi HY (2009). Merkel cells are essential for light-touch responses. Science 324, 1580–1582. [PubMed: 19541997]

Martemyanov KA, and Sampath AP (2017). The Transduction Cascade in Retinal ON-Bipolar Cells: Signal Processing and Disease. Annu Rev Vis Sci 3, 25–51. [PubMed: 28715957]

Matsushita N, Okada H, Yasoshima Y, Takahashi K, Kiuchi K, and Kobayashi K (2002). Dynamics of tyrosine hydroxylase promoter activity during midbrain dopaminergic neuron development. J Neurochem 82, 295–304. [PubMed: 12124430]

Mayer ML, and Westbrook GL (1983). A voltage-clamp analysis of inward (anomalous) rectification in mouse spinal sensory ganglion neurones. J Physiol 340, 19–45. [PubMed: 6887047]

McLachlan EM, Janig W, Devor M, and Michaelis M (1993). Peripheral nerve injury triggers noradrenergic sprouting within dorsal root ganglia. Nature 363, 543–546. [PubMed: 8505981]

Merkel F (1875). Tastzellen und Tastkörperchen bei den Hausthieren und beim Menschen. Archiv für Mikroskopische Anatomie 11, 636–652.

Mihara M, Hashimoto K, Ueda K, and Kumakiri M (1979). The specialized junctions between Merkel cell and neurite: an electron microscopic study. J Invest Dermatol 73, 325–334. [PubMed: 501131]

Moehring F, Cowie AM, Menzel AD, Weyer AD, Grzybowski M, Arzua T, Geurts AM, Palygin O, and Stucky CL (2018). Keratinocytes mediate innocuous and noxious touch via ATP-P2X4 signaling. Elife 7.

Molinoff PB, and Axelrod J (1971). Biochemistry of catecholamines. Annu Rev Biochem 40, 465–500. [PubMed: 4399447]

Morita T, McClain SP, Batia LM, Pellegrino M, Wilson SR, Kienzler MA, Lyman K, Olsen AS, Wong JF, Stucky CL, et al. (2015). HTR7 Mediates Serotonergic Acute and Chronic Itch. Neuron 87, 124–138. [PubMed: 26074006]

Morrison KM, Miesegaes GR, Lumpkin EA, and Maricich SM (2009). Mammalian Merkel cells are descended from the epidermal lineage. Dev Biol 336, 76–83. [PubMed: 19782676]

Nakamura F, and Strittmatter SM (1996). P2Y1 purinergic receptors in sensory neurons: contribution to touch-induced impulse generation. Proc Natl Acad Sci U S A 93, 10465–10470. [PubMed: 8816824]

Nakamura T, and Gold GH (1987). A cyclic nucleotide-gated conductance in olfactory receptor cilia. Nature 325, 442–444. [PubMed: 3027574]

Niu J, Vysochan A, and Luo W (2014). Dual innervation of neonatal Merkel cells in mouse touch domes. PLOS One 9, e92027. [PubMed: 24637732]

Nunzi MG, Pisarek A, and Mugnaini E (2004). Merkel cells, corpuscular nerve endings and free nerve endings in the mouse palatine mucosa express three subtypes of vesicular glutamate transporters. J Neurocytol 33, 359–376. [PubMed: 15475690]

Pang Z, Sakamoto T, Tiwari V, Kim YS, Yang F, Dong X, Guler AD, Guan Y, and Caterina MJ (2015). Selective keratinocyte stimulation is sufficient to evoke nociception in mice. Pain 156, 656–665. [PubMed: 25790456]

Pennington JM, Millar J, CP LJ, Owesson CA, McLaughlin DP, and Stamford JA (2004). Simultaneous real-time amperometric measurement of catecholamines and serotonin at carbon fibre ‘dident’ microelectrodes. J Neurosci Methods 140, 5–13. [PubMed: 15589328]

Press D, Mutlu S, and Guclu B (2010). Evidence of fast serotonin transmission in frog slowly adapting type 1 responses. Somatosens Mot Res 27, 174–185. [PubMed: 20937000]

R Development Core Team (2010). R: A language and environment for statistical computing (Vienna, Austria: R Foundation for Statistical Computing).

Ramirez-Franco JJ, Munoz-Cuevas FJ, Lujan R, and Jurado S (2016). Excitatory and Inhibitory Neurons in the Hippocampus Exhibit Molecularly Distinct Large Dense Core Vesicles. Front Cell Neurosci 10, 202. [PubMed: 27630542]

Rausl A, Nordlind K, and Wahlgren CF (2013). Pruritic and vascular responses induced by serotonin in patients with atopic dermatitis and in healthy controls. Acta Derm Venereol 93, 277–280. [PubMed: 23165739]

Reinisch CM, and Tschachler E (2005). The touch dome in human skin is supplied by different types of nerve fibers. Ann Neurol 58, 88–95. [PubMed: 15984029]

Rich TC, Fagan KA, Nakata H, Schaack J, Cooper DM, and Karpen JW (2000). Cyclic nucleotide-gated channels colocalize with adenylyl cyclase in regions of restricted cAMP diffusion. J Gen Physiol 116, 147–161. [PubMed: 10919863]

Rose MF, Ren J, Ahmad KA, Chao HT, Klisch TJ, Flora A, Greer JJ, and Zoghbi HY (2009). Math1 is essential for the development of hindbrain neurons critical for perinatal breathing. Neuron 64, 341–354. [PubMed: 19914183]

Rosenbaum DM, Rasmussen SG, and Kobilka BK (2009). The structure and function of G-protein-coupled receptors. Nature 459, 356–363. [PubMed: 19458711]

Salzer I, Gantumur E, Yousuf A, and Boehm S (2016). Control of sensory neuron excitability by serotonin involves 5HT2C receptors and Ca(2+)-activated chloride channels. Neuropharmacology 110, 277–286. [PubMed: 27511837]

Sato J, and Perl ER (1991). Adrenergic excitation of cutaneous pain receptors induced by peripheral nerve injury. Science 251, 1608–1610. [PubMed: 2011742]

Schneider CA, Rasband WS, and Eliceiri KW (2012). NIH Image to ImageJ: 25 years of image analysis. Nat Methods 9, 671–675. [PubMed: 22930834]

Shih JC, Chen K, and Ridd MJ (1999). Monoamine oxidase: from genes to behavior. Annu Rev Neurosci 22, 197–217. [PubMed: 10202537]

Shroyer NF, Helmrath MA, Wang VY, Antalffy B, Henning SJ, and Zoghbi HY (2007). Intestine-specific ablation of mouse atonal homolog 1 (Math1) reveals a role in cellular homeostasis. Gastroenterology 132, 2478–2488. [PubMed: 17570220]

Stewart WC, and Castelli WP (1996). Systemic side effects of topical beta-adrenergic blockers. Clin Cardiol 19, 691–697. [PubMed: 8874987]

Tachibana T, and Nawa T (2002). Recent progress in studies on Merkel cell biology. Anat Sci Int 77, 26–33. [PubMed: 12418081]

Tachibana T, and Nawa T (2005). Immunohistochemical reactions of receptors to met-enkephalin, VIP, substance P, and CGRP located on Merkel cells in the rat sinus hair follicle. Arch Histol Cytol 68, 383–391. [PubMed: 16505584]

Torebjörk E, Wahren L, Wallin G, Hallin R, and Koltzenburg M (1995). Noradrenaline-evoked pain in neuralgia. Pain 63, 11–20. [PubMed: 8577481]

Toyoshima K, and Shimamura A (1991). Uranaffin reaction of Merkel corpuscles in the lingual mucosa of the finch, Lonchula striata var. domestica. J Anat 179, 197–201. [PubMed: 1726218]

Urtikova N, Berson N, Van Steenwinckel J, Doly S, Truchetto J, Maroteaux L, Pohl M, and Conrath M (2012). Antinociceptive effect of peripheral serotonin 5-HT2B receptor activation on neuropathic pain. Pain 153, 1320–1331. [PubMed: 22525520]

Usoskin D, Furlan A, Islam S, Abdo H, Lonnerberg P, Lou D, Hjerling-Leffler J, Haeggstrom J, Kharchenko O, Kharchenko PV, et al. (2015). Unbiased classification of sensory neuron types by large-scale single-cell RNA sequencing. Nat Neurosci 18, 145–153. [PubMed: 25420068]

Van Buskirk EM (1980). Adverse reactions from timolol administration. Ophthalmology 87, 447–450. [PubMed: 7402590]

Van Keymeulen A, Mascre G, Youseff KK, Harel I, Michaux C, De Geest N, Szpalski C, Achouri Y, Bloch W, Hassan BA, et al. (2009). Epidermal progenitors give rise to Merkel cells during embryonic development and adult homeostasis. J Cell Biol 187, 91–100. [PubMed: 19786578]

Vielkind U, Sebzda MK, Gibson IR, and Hardy MH (1995). Dynamics of Merkel cell patterns in developing hair follicles in the dorsal skin of mice, demonstrated by a monoclonal antibody to mouse keratin 8. Acta Anat (Basel) 152, 93–109. [PubMed: 7544943]

Weihe E, Hartschuh W, Schafer MK, Romeo H, and Eiden LE (1998). Cutaneous Merkel cells of the rat contain both dynorphin A and vesicular monoamine transporter type 1 (VMAT1) immunoreactivity. Can J Physiol Pharmacol 76, 334–339. [PubMed: 9673797]

Wellnitz SA, Lesniak DR, Gerling GJ, and Lumpkin EA (2010). The regularity of sustained firing reveals two populations of slowly adapting touch receptors in mouse hairy skin. J Neurophysiol 103, 3378–3388. [PubMed: 20393068]

Westlund KN, and Coulter JD (1980). Descending projections of the locus coeruleus and subcoeruleus/medial parabrachial nuclei in monkey: axonal transport studies and dopamine-beta-hydroxylase immunocytochemistry. Brain Res 2, 235–264. [PubMed: 7470856]

Wilson SR, The L, Batia LM, Beattie K, Katibah GE, McClain SP, Pellegrino M, Estandian DM, and Bautista DM (2013). The epithelial cell-derived atopic dermatitis cytokine TSLP activates neurons to induce itch. Cell 155, 285–295. [PubMed: 24094650]

Woo SH, Ranade S, Weyer AD, Dubin AE, Baba Y, Qiu Z, Petrus M, Miyamoto T, Reddy K, Lumpkin EA, et al. (2014). Piezo2 is required for Merkel-cell mechanotransduction. Nature 509, 622–626. [PubMed: 24717433]

Woodbury CJ, and Koerber HR (2007). Central and peripheral anatomy of slowly adapting type I low-threshold mechanoreceptors innervating trunk skin of neonatal mice. J Comp Neurol 505, 547–561. [PubMed: 17924532]

Yamamoto M, Wada N, Kitabatake Y, Watanabe D, Anzai M, Yokoyama M, Teranishi Y, and Nakanishi S (2003). Reversible suppression of glutamatergic neurotransmission of cerebellar granule cells in vivo by genetically manipulated expression of tetanus neurotoxin light chain. J Neurosci 23, 6759–6767. [PubMed: 12890769]

Yau KW, and Baylor DA (1989). Cyclic GMP-activated conductance of retinal photoreceptor cells. Annu Rev Neurosci 12, 289–327. [PubMed: 2467600]

Yu CR, Power J, Barnea G, O'Donnell S, Brown HE, Osborne J, Axel R, and Gogos JA (2004). Spontaneous neural activity is required for the establishment and maintenance of the olfactory sensory map. Neuron 42, 553–566. [PubMed: 15157418]

Zeitz KP, Guy N, Malmberg AB, Dirajlal S, Martin WJ, Sun L, Bonhaus DW, Stucky CL, Julius D, and Basbaum AI (2002). The 5-HT3 subtype of serotonin receptor contributes to nociceptive processing via a novel subset of myelinated and unmyelinated nociceptors. J Neurosci 22, 1010–1019. [PubMed: 11826129]

Zhang Y, Narayan S, Geiman E, Lanuza GM, Velasquez T, Shanks B, Akay T, Dyck J, Pearson K, Gosgnach S, et al. (2008). V3 spinal neurons establish a robust and balanced locomotor rhythm during walking. Neuron 60, 84–96. [PubMed: 18940590]

Zhou FW, Dong HW, and Ennis M (2016). Activation of beta-noradrenergic receptors enhances rhythmic bursting in mouse olfactory bulb external tufted cells. J Neurophysiol 116, 2604–2614. [PubMed: 27628203]

Highlights

- Epidermal Merkel cells form adrenergic synapses with Aβ mechanosensory afferents.
- Norepinephrine directly activates action potentials in Merkel-cell afferents.
- Merkel cells employ SNARE-dependent vesicular release to excite tactile afferents.
- Neuronal β_2-adrenergic receptors are required for slowly adapting type I responses

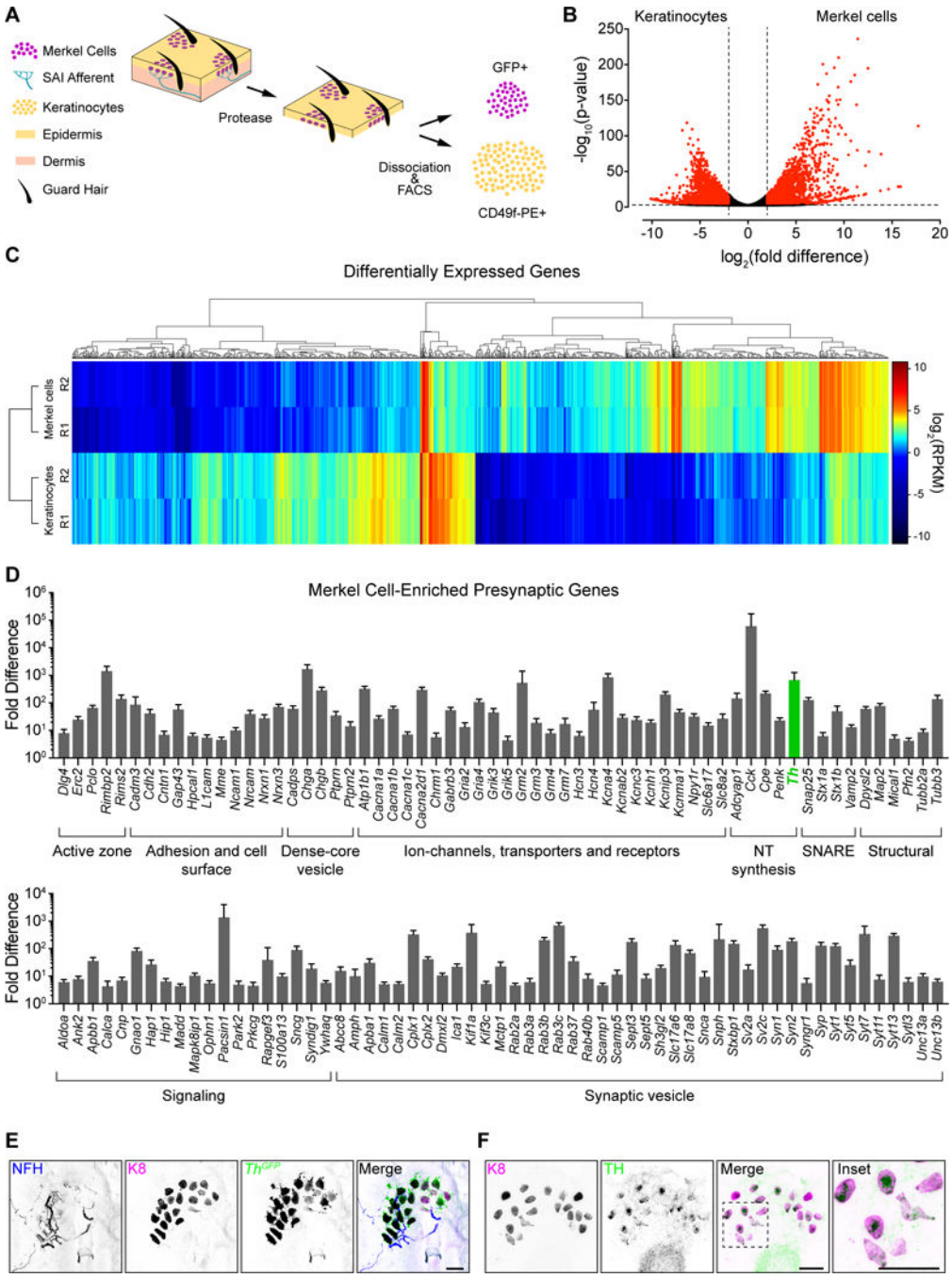

Figure 1. Merkel cells are presynaptic, catecholaminergic cells.

A. Epidermal cell purification strategy [n=2 fluorescence-activated cell sorting (FACS) purifications from n≥2, 7–8-week *Atoh1*^{GFP} mice each]. **B.** Volcano plot of genes differentially expressed between Merkel cells and keratinocytes. Dashed lines indicate $\log_2$(fold difference)≥2 and P_{adj}<0.01 for differential expression (red, above threshold; black, below threshold). **C.** Hierarchical clustering of differentially expressed genes. Rows represent RNA-seq replicates (R1/R2). Dendrograms show expression profiles of genes (top) and replicates (left). RPKM, reads per kilobase of exon per million reads mapped. Genes

with RPKM<2 across all samples are not displayed. **D.** Presynaptic genes enriched in Merkel cells are grouped according to functional class. Log_2 transformed fold difference is plotted. **E.** Axial projection of a whole-mount touch dome from an adult Th^{GFP} mouse stained with antibodies against NFH (blue in merge), K8 (magenta) and GFP (green). **F.** Maximum projection of a touch dome in an epidermal peel stained with antibodies against K8 (magenta) and TH (green). Scale bars, 25 μm. See also Figure S1 and Tables S1 and S2.

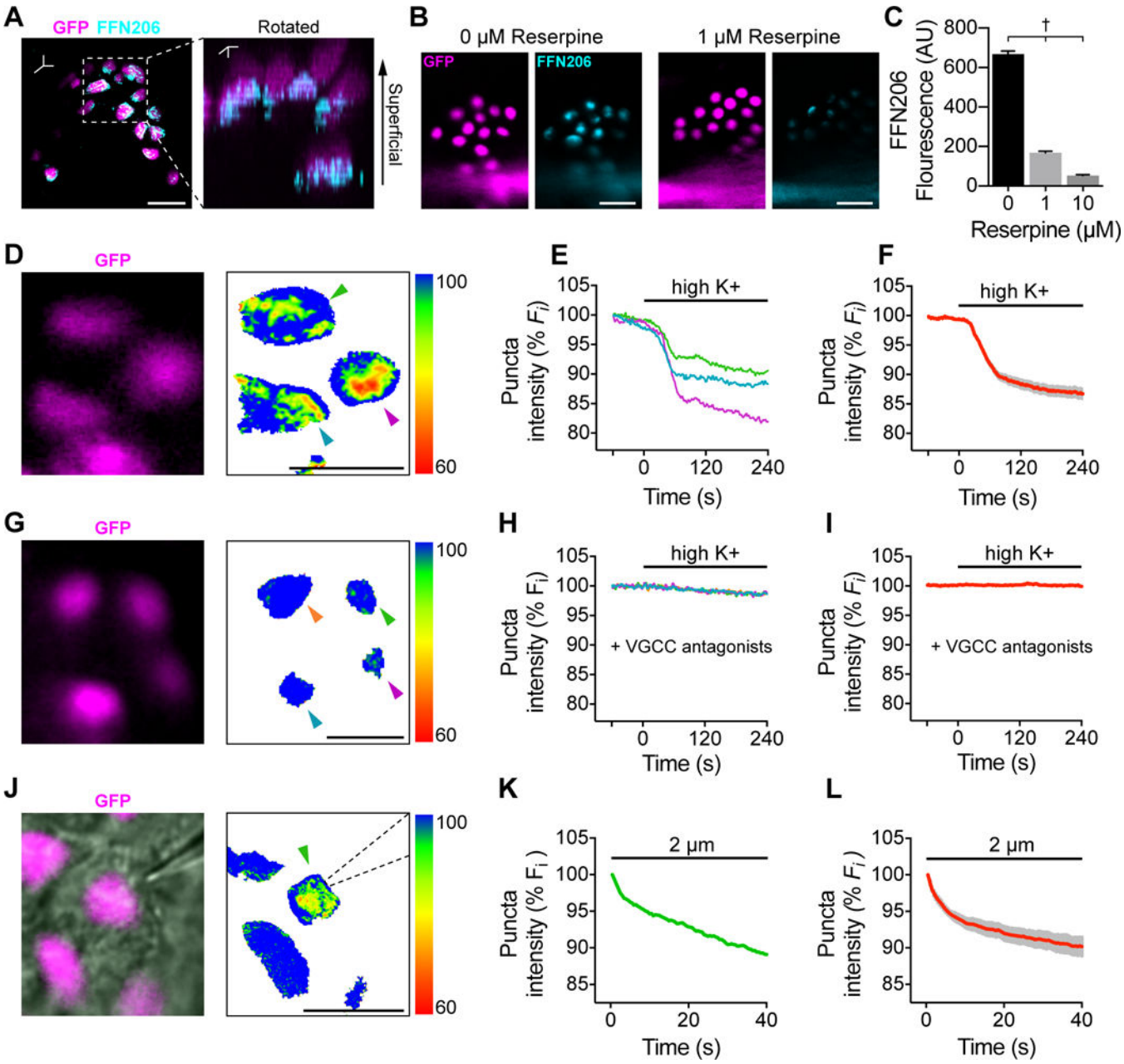

Figure 2. Merkel cells mediate uptake and activity-evoked release of fluorescent neurotransmitters.

A. Left, Merkel cells (magenta) loaded with FFN206 (1 μM, cyan) in an epidermal peel preparation from an *Atoh1*^{nGFP} mouse, which expresses a nuclear localized GFP driven by *Atoh1* enhancer elements. Right, three-dimensional reconstruction, rotated. Images are representative of *n*=9 touch domes, 2 animals. **B.** FFN206 loading in *Atoh1*^{nGFP} Merkel cells co-incubated with vehicle (left) or 1 μM reserpine (right). **C.** Quantification of FFN206 loading (background subtracted fluorescence, one-way ANOVA, Tukey's post-hoc; †P<0.0001 for all comparisons; mean±SEM; *n*=205–331 Merkel cells per group, 2 animals). (**D–I**). FFN206-loaded Merkel cells stimulated with high K^+ Ringer's solution. Pseudocolor images show the ratio of FFN206 fluorescence to baseline 240 s after application of high K^+

Ringer's solution. Scale indicates percent decrease in pixel intensity from baseline. **D.** *Atoh1*^{nGFP}- positive Merkel cells (magenta). **E.** Baseline normalized, intensity versus time traces of puncta indicated by arrowheads in (**D**). Black bar, high K^+ application. **F.** Mean (red) ± SEM (gray) of puncta that showed release in response to depolarization (n=40 cells, 3 animals). (**G–I**). Merkel cells loaded with FFN206, incubated with VGCC antagonists (10 μM nimodipine + 10 μM ω-conotoxin MVII-C), and stimulated high K+ Ringer's solution. **G.** *Atoh1*^{GFP}-positive Merkel cells (magenta) and pseudocolor difference image. **H.** Baseline normalized, intensity versus time traces of puncta indicated by arrowheads in (**G**). Black bar, high K^+ application. **I.** Mean (red) SEM (gray) of summary data (n=69 Merkel cells, 3 mice). (**J–L**). Merkel cells loaded with FFN206 and stimulated with displacement. **J.** Left, Merkel cells (*Atoh1*^{nGFP}; magenta). Right, ratio of FFN206 fluorescence to baseline 40 s after the onset of displacement. Dashed lines outline the stimulus probe. **K.** Baseline normalized, intensity versus time traces of puncta indicated by the arrowhead in (**J**). Black bar, mechanical stimulation. **L.** Mean (red) SEM (gray) of mechanically evoked FFN206 release (n=6 Merkel cells, 3 animals). Scale bars, 20 μm. See also Figure S2 and Videos S1, S2, and S3.

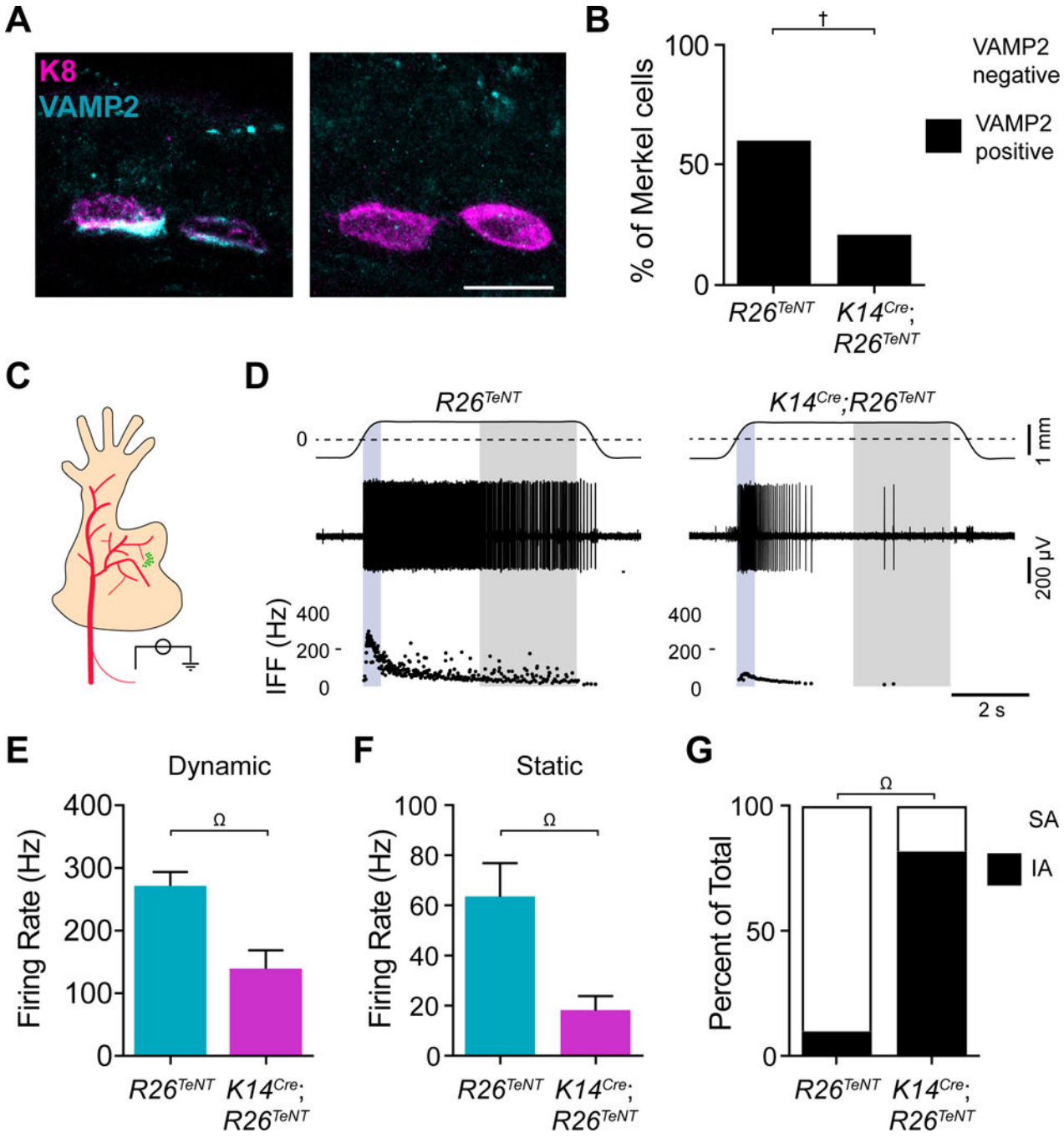

Figure 3. Merkel cells employ SNARE-dependent vesicular release to mediate SAI responses.

A. Images of Merkel cells (magenta) and VAMP2 (cyan) immunoreactivity from littermate-control (*R26*^{TeNT}) and TeNT-expressing mice (*K14*^{Cre};*R26*^{TeNT}; scale bar, 10 μm). **B.** Quantification of Merkel cells with detectable VAMP2 immunoreactivity (cyan; two-sided Fisher's exact test, $^{\dagger}P<0.0001$; n=149–161 cells from 3 mice per group). **C.** Schematic of *ex vivo* skin-nerve recording preparation (saphenous nerve, red; FM1–43-labeled touch dome, green). Receptive fields of touch-dome afferents were identified by FM1–43 fluorescence in epidermal-side up recordings. **D.** Recordings from touch-dome afferents from littermate-

control (left) and $K14^{Cre};R26^{TeNT}$ (right) mice. Top traces, displacement (dashed lines, point of skin contact). Middle traces, action potential trains. Bottom, instantaneous firing frequency (IFF) plots [blue region, dynamic (ramp) phase; gray region, static (late hold) phase]. (**E–G**). Maximal touch-evoked responses from littermate-control (cyan) and $K14^{Cre};R26^{TeNT}$ (magenta). Peak dynamic firing rate (**E**) and mean static firing rate (**F**). Mean±SEM; two-tailed Mann-Whitney test, $^{\Omega}$P<0.005. **G.** Units were classified as slowly adapting (SA, white) if spikes were observed throughout the 5-s hold phase in ≥75% of stimulus presentations, otherwise they were classified as intermediately adapting (IA, black; two-sided Fisher's exact test, $^{\Omega}$P<0.005; n=10–11 fibers, 9 mice per group). See also Figures S3 and S4.

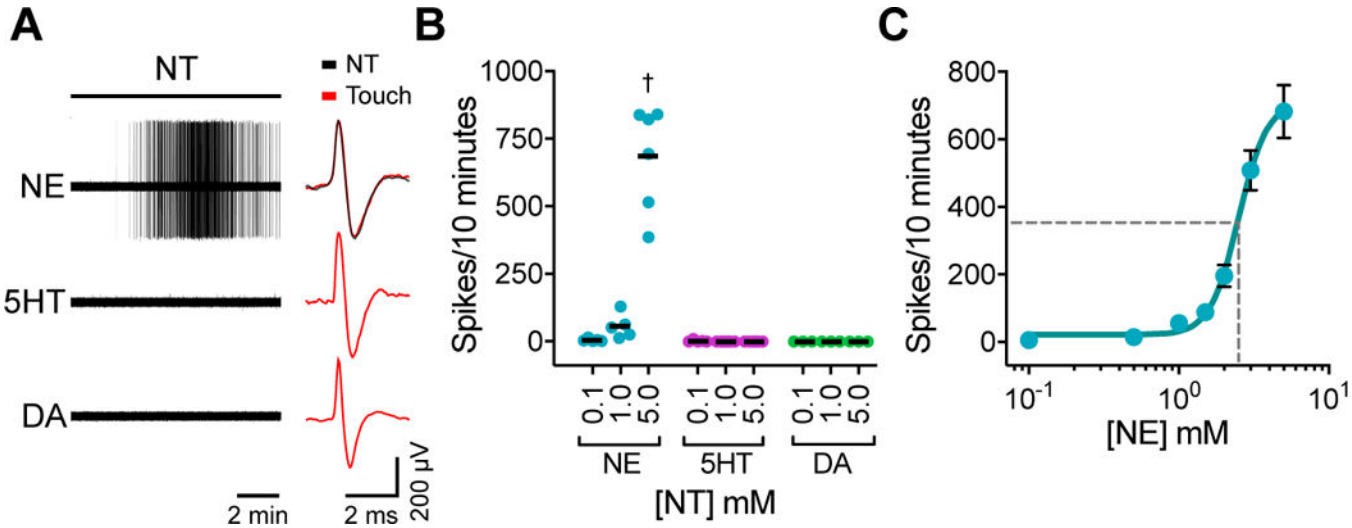

Figure 4. Norepinephrine excites action potentials in Merkel-cell afferents.

(**A–C**). Norepinephrine (NE), serotonin (5HT), or dopamine (DA) was applied to receptive fields of touch-dome afferents in *ex vivo* skin-nerve recordings. Receptive fields of touch-dome afferents were identified by FM1–43 fluorescence and then preparations were flipped dermis-side up for receptive-field perfusion. **A.** Left, neurotransmitter-evoked action potentials. Right, comparison of touch-evoked and neurotransmitter-evoked spike waveforms. Black bar indicates perfusion of 5-mM neurotransmitter (10 min). **B.** Total spikes evoked by each neurotransmitter at 0.1 mM, 1.0 mM or 5.0 mM (two-way ANOVA with Tukey's post-hoc, $^{\dagger}P<0.0001$; $n_{NE}=8$ units, 8 mice; $n_{5HT}=9$ units, 9 mice; $n_{DA}=4$ units, 4 mice; lines, medians). **C.** Agonist-response relationship of NE-evoked spikes in Merkel-cell afferents (mean±SEM; $EC_{50}=2.5$ mM; $R^2=0.89$; $n=11$ units, 9 mice).

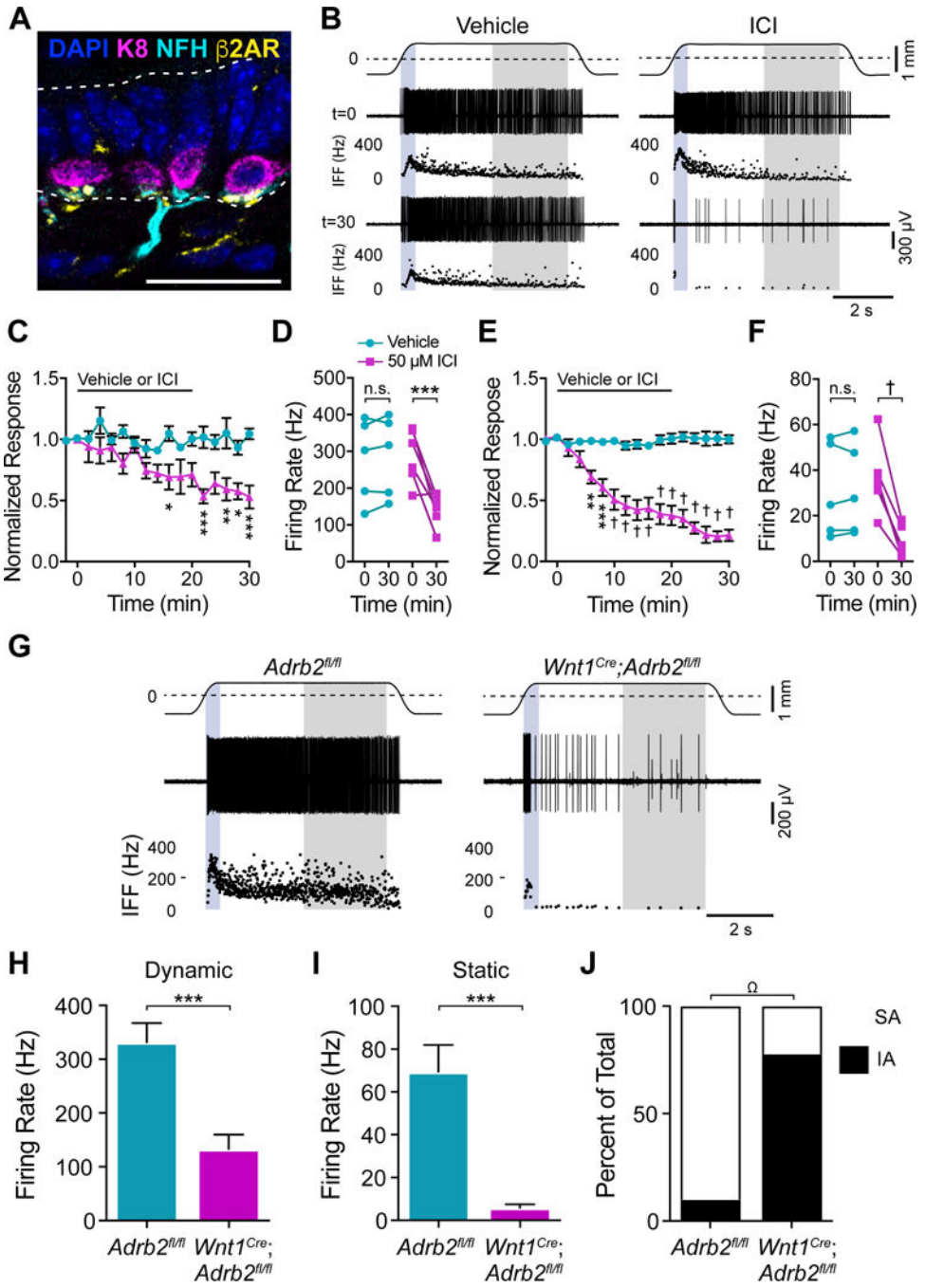

Figure 5. Neuronal β_2ARs are required for touch-evoked SAI responses.

A. Merkel cells (K8, magenta), Merkel-cell afferent (NFH, cyan), and β_2AR (yellow) immunoreactivity in adult mouse back skin (scale bar, 25 μm). **B.** Recordings from Merkel-cell afferents and corresponding IFF plots before and 30 min after treatment with vehicle or 50 μM ICI 118,551. Traces and shading as in Fig. 3D. (**C–F**). Peak dynamic firing rate (**C, D**) and mean static firing rates (**E, F**) from afferents treated with vehicle (cyan) or 50 μM ICI 118,551 (magenta) and stimulated at 2-min intervals. **C, E.** Firing rates at each time point was normalized to t=0 to average responses across units (mean±SEM). Black bar indicates

time of vehicle or 50 μM ICI 118,551 application. **D, F**. Firing rates of all units before (t=0) and after (t=30) treatment with vehicle or 50 μM ICI 118,551. Two-way matched ANOVA with Sidak's post-hoc; *P<0.05, **P<0.01, ***P<0.001, †P<0.0001; n=5–6 units from 5–6 mice per group. **G.** Recordings from Merkel-cell afferents from littermate control (left) and *Wnt1*^{Cre};*Adrb2*$^{fl/fl}$ (right) mice. (**H–J**). Maximal touch-evoked responses from littermate-control (cyan) and *Wnt1*^{Cre};*Adrb2*$^{fl/fl}$ (magenta) units. **H.** Peak dynamic firing rate. **I.** Mean static firing rate (two-tailed Student's *t* test, ***P<0.001; mean±SEM). **J.** Proportion of Merkel-cell afferents with SA (white) versus IA firing patterns (black); two-sided Fisher's exact test, $^{\Omega}$P<0.005; n=9–10 units, 9 mice per group). See also Figure S5.

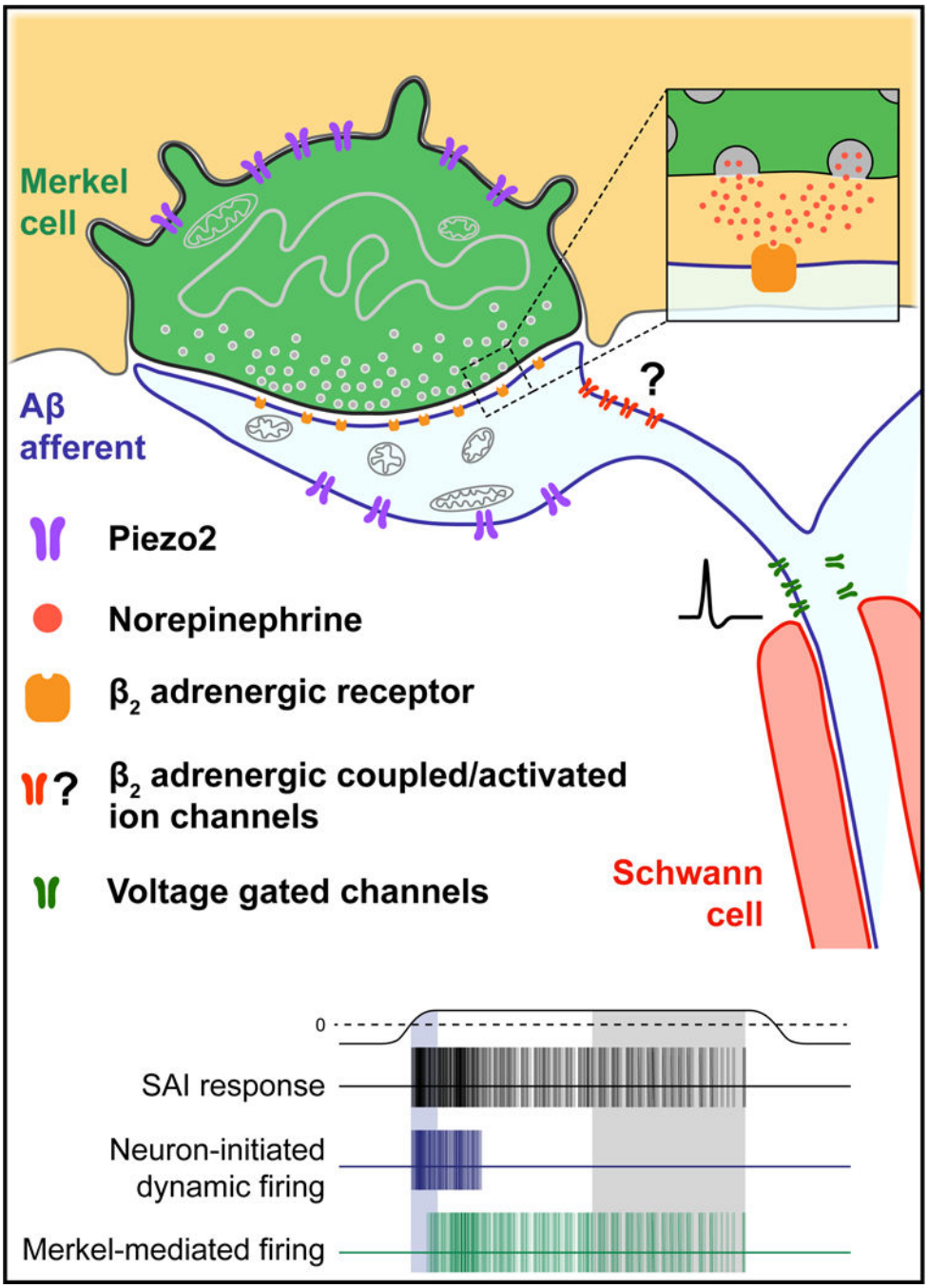

Figure 6. Model for adrenergic synaptic transmission at the Merkel cell-neurite complex.

Touch activates cation influx through Piezo2 channels to depolarize Merkel cells and their afferents. During dynamic stimuli, neuronal Piezo2 stimulates action potential firing. Merkel-cell depolarization results in voltage-dependent calcium channel activation, and SNARE-mediated release of norepinephrine. Norepinephrine binds to β_2 adrenergic receptors on SAI afferents, which increases dynamic firing rates and initiates action potentials during static stimulation. See also Figure S6.